PERFORMANCE OF A FLAT PLATE SOLAR ENERGY COLLECTOR

By

Gardjito

A THESIS

Submitted to
Michigan State University
in partial fulfillment of the requirements
for the degree of

MASTER OF SCIENCE

Agricultural Engineering Department

1980

ABSTRACT

PERFORMANCE OF A FLAT PLATE
SOLAR ENERGY COLLECTOR

By

Gardjito

A solar energy utilization research project has been conducted by the Agricultural Engineering and Poultry Science Departments of Michigan State University. A low, cost flat-plate, single air-pass solar collector was constructed to provide supplemental heating for a 5,000 bird poultry laying house during winter months, and to supply heat for excreta drying during summer. The collector was 3.05 m by 30.62 m in size, faced south, and tilted at 60^o from the horizontal plane.

An experiment was conducted during the months of May through August, 1978 to evaluate the performance of the solar collector under realistic field conditions. The collector was operated with four air flow rates of 0.32, 0.48, 0.53, and 0.64 m^3/min./m^2. The results indicated that within the range of the air flow rates observed the collector efficiency increased linearly with increased air flow. There was essentially a direct relationship between the volumetric air flow rate and the instantaneous efficiency. Under a constant air flow, the collector efficiency also increased with increased insolation.

Other results from the performance test indicated that the daily average efficiency of the collector ranged from 33 to 73 percent and the total daily heat collection ranged from 1,949 to 7,446 kJ/m^2 depending on the air flow rate and weather conditions. The maximum instantaneous efficiency of the collector was 81 percent.

Approved:

Merle L Esmay
Major Professor

Richard H Hiller
Department Chairman

ACKNOWLEDGEMENTS

The author wishes to express sincere gratitude to Dr. Merle L. Esmay (Agricultural Engineering Department) for his advise, encouragement, suggestions, and patience in guiding during the course of this study and for serving as the major professor.

Appreciation is extended to Dr. C. A. Rotz (Agricultural Engineering Department) and Dr. C. R. St. Clair (Mechanical Engineering Department) for their invaluable guidance. Appreciation is also extended to his fellow students F. W. Hall and R. Haney for their significant help and cooperation.

Finally, thanks to Mrs. Cindy Jennings for her diligence in typing this manuscript.

TABLE OF CONTENTS

Page

LIST OF TABLES

LIST OF FIGURES

I. INTRODUCTION

1.1 Background

Until a few years ago, proposals for using the sun's energy on a significant scale were likely to be received with skepticism. During the last several years, however, the increasing cost of conventional fuels, the political uncertainties related to the supply of petroleum, and the problems associated with electric-energy generation from nuclear sources have modified this skepticism dramatically. Solar energy shows promise of becoming a dependable energy source without new requirements of a highly technical and specialized nature for its widespread utilization. In addition, there appear to be no significant polluting effects from its use (Kreider and Kreith, 1975).

Many topics of research related to utilization of solar energy in agriculture have been conducted. Solar energy can be utilized for supplemental heating of egg production housing during winter months, in-house excreta drying during summer months, water heating for industrial and domestic uses, grain drying, and home heating (Hall, et al, 1977; Edwards, 1977).

Methods of solar energy collection range from active, mechanical, solar thermal collectors, to photoelectrical devices, to windmills, to fully passive collection systems. While the heat from a solar collector can be used in conventional ways, there are a number of factors that make application of solar heat collectors challenging.

The amount of solar energy available is very large but has the disadvantage of being intermittent and relatively low in intensity. Not only is there the nightly disappearance of the sun and the seasonal variation of the length of the day, but there is the unpredictable effect of local meteorological conditions (like clouds) upon the availability of solar energy. Unlike conventional heaters, solar heaters cannot be turned on whenever desired. With a solar heating system, an auxiliary heater is almost universally required even when thermal storage is employed for continuous utilization of the solar energy. Thus the solar collector is currently used to augment or stretch our supplies of fossil, nuclear, or biological fuel, and not to replace the systems.

One of the low cost and easy to construct solar thermal collectors is a simple flat-plate collector. An air-cooled flat-plate collector can be used especially for drying and space conditioning. The use of air as a heat transfer fluid has the advantage of being non-corrosive and less costly. When warm air is the desired goal, the non-corrosive nature of air permits the use of very inexpensive materials, and the prospect of a leak developing inadvertently poses no threat to property.

The performance of a solar collector is based upon its efficiency in collecting heat. A method of testing and rating solar collectors on the basis of thermal performance has been developed by The National Bureau of Standards (Hill et al., 1976). The procedure is to operate the collector on a test stand under steady conditions. The solar radiation, windspeed, and the ambient and inlet fluid temperature are all maintained essentially constant for a period long enough so that the fluid outlet temperature and the useful energy gain do not change appreciably with time.

In practical operations, a solar collector heating system operates over a wide range of conditions. The local meteorological conditions as well as the collector design affect the collector performance. In the utilization of a solar energy collector for any purpose, a test of performance under realistic conditions is important.

1.2 Objective

Research on solar energy utilization for supplemental heating of egg production housing in the northern states during winter months has been conducted by the Agricultural Engineering and Poultry Science Departments of Michigan State University. A low cost, flat-plate, single air-pass solar collector was constructed to provide supplemental heating for a 5,000 bird poultry laying house.

This thesis experiment was conducted to evaluate the performance of the solar collector used in the supplemental heating research project. The specific objectives are:

a. to determine the effect of air-flow rate on the efficiency of the collector
b. to examine other factors influencing the performance of the collector.

II. LITERATURE REVIEW

2.1 Utilization of Solar Energy in Agriculture

The utilization of solar energy in agriculture has been studied by many investigators. The experimental heat collection systems were mostly of the flat-plate type that used either water or air as heat carrying medium. The air type solar collectors have been used mainly for drying and space conditioning.

Kline (1977) studied the utilization of solar collectors for low temperature grain drying. The performance of twelve different collectors were investigated. Tests were conducted in Ames, Iowa, during the fall and spring grain drying seasons to measure the amount of solar energy that could be collected by the different types of collectors. The collectors, except for one, were of the flat-plate type with air as the heat exchange medium. The solar collector efficiencies ranged from 14 to 80 percent. The tests also indicated that the collectors with high performance could collect approximately 1,500 Btu per day per square foot (3,672.8 Kcal per day per square meter) of collector surface area on sunny days in spring and fall 1976.

Other investigators worked on utilization of solar energy for space conditioning. Spillman (1976) and DeShazer et al, (1976) studied the supplemental heating by solar energy for swine buildings.

The supplemental heating for poultry housing and manure drying were investigated by Horsfield and DeBaerdemaeker (1976), Reece (1976), Brown and Forbes (1976), Merkel et al, (1976) Hall et al, (1977), and Forbes and McClendon (1977). The solar heating systems for greenhouses were studied by Baierd et al, (1977), Mears et al, (1977), and Milburn et al, (1977).

2.2 Solar Radiation

One of the difficulties involved in the use of solar energy is the fact that the incoming solar radiation at the surface of the earth is a quite random quantity, predictable only in a statistical way, because of the random nature of the weather (deWinter, 1975). Furthermore, although solar energy is immense in quantity, it has the disadvantage of being intermittently available and relatively low in intensity (Becker and Boyd, 1957).

2.2.1 Solar Constant

The solar constant is the energy incident upon a unit area located at a mean distance of the earth from the sun and oriented perpendicular to the sun's rays beyond the atmosphere. Outside the earth's atmosphere the solar constant is quite predictable. According to Thekaekara (1973), when the earth is furthest away from the sun the incoming flux on a surface normal to the sun's rays is about 130.9 milliwatts/cm^2, when it is closest about 139.9 mW/cm^2, and the average is about 135.3 mW/cm^2 (429.1 Btu/hr. $ft.^2$). However, the average value of the solar constant has fluctuated significantly during the last 30 years or more, and is now back very close to the level it was thought to have about 100 years ago by John Ericsson, who concluded in 1876 that the solar constant was 134.5 mW/cm^2 (deWinter, 1975). Abbot, based on extensive measurements made by the Smithsonian Institution during the first decade of this century, arrived at a value of 134.6 mW/cm^2 (Thekaekara, 1965). Because of an error thought to exist in Abbot's results, Moon (1940) adjusted the value downward to 132.2 mW/cm^2, and this value became widely accepted in the 1940s. Based on the latest measurements by Thekaekara (1973) the solar constant value is back to 135.3 mW/cm^2, quite close to the value of Ericsson's.

The position of the sun depends on the time of the day and year. The daily solar motion is caused by the constant rotational speed of the earth, and the somewhat variable speed of the earth around the sun. The seasonal solar motion is due to the fact that the axis of the earth is not perpendicular to the plane of the ecliptic (the plane in which the earth moves around the sun), but has a tilt angle about 23.5 degree (deWinter, 1975; and ASHRAE Handbook of Fundamentals, 1977). This causes the sun to have a varying declination (the angle between the earth - sun line and the equatorial plane) during the year, and causes the changing seasons, with their unequal periods of daylight and darkness. Because the earth's orbit is slightly elliptical and the extraterrestrial radiation intensity varies inversely as the square of the earth - sun distance, it is maximum (139.19 mW/cm^2) on December 21, when the earth is closest to the sun, and is minimum (130.9 mW/cm^2) on June 21, when the earth - sun distance reaches its maximum.

2.2.2 Effect of Atmospheric Constituents on Solar Energy

Once the solar energy enters the atmosphere, depletion of the direct beam takes place by scattering and absorption. Scattering is caused primarily by air molecules, dust, and to certain extent by water vapor and droplets along the path of the sun's rays to the surface of the earth. The principal absorbing agents are water vapor, ozone, and cloud particles. This series of phenomena can appreciably reduce the radiation (Kondratyev, 1969). Sun-light entering the atmosphere at an angle is bent downward due to the higher index of refraction of the denser air closer to the earth. The sun is hence always lower in the sky than it appears to be. The effect is, however, small except at dusk and dawn, and the size of the sun is not affected.

The absorption process by gases in the atmosphere generally affects specific wave length bands, so that the radiation reaching the earth has been very significantly depleted in many parts of the spectrum (Threlkeld and Jordan, 1957). Most ultraviolet solar radiation is absorbed by the ozone in the upper atmosphere, while part of the radiation in the shortwave portion of the spectrum is scattered by air molecules, imparting the familiar blue color to the sky (ASHRAE Handbook of Fundamentals, 1977). Water vapor in the lower atmosphere causes the characteristic absorption bands observed in the solar spectrum at sea level. For a solar altitude of 30 degrees, the spectrum of the sun's direct radiation on a clear day at sea level shows less than 3 percent of the total energy in the ultraviolet, 44 percent in the visible region, and the remaining 53 percent in the infrared. The maximum intensity comes at 0.50 um, and there is virtually no solar energy at wave lengths beyond 2.2 um.

Some shortwave radiation scattered by air molecules and dust reaches the earth in the form of diffuse radiation. Since this diffuse radiation comes from all parts of the sky, its intensity is difficult to predict and it is subject to wide variation as moisture and dust content of the atmosphere change throughout any given day. On a completely overcast day, the diffuse component accounts for all solar radiation reaching the earth. The total shortwave radiation reaching a terrestrial surface is the sum of the direct solar radiation, the diffuse sky radiation, and the solar radiation reflected from surrounding surfaces. The intensity of the direct component is the product of the direct normal irradiation and the cosine of the angle of incidence between the incoming solar rays and a line normal to the surface. Method of computing solar radiation or insolation can be found from ASHRAE Handbook of Fundamentals (1977) or many other sources of literature.

2.2.3 Insolation Values at the Surface of the Earth

Weather and insolation can change drastically in perhaps 5 miles or less due to locations, i.e., closeness to mountains, coasts, or other such influences. There are probably very few locations in which there are no significant changes in 50 miles (deWinter, 1975). Good results on the insolation measurements are required in order to evaluate the performance of flat-plate solar collectors properly.

A sufficiently long series of instanteneous measurements is necessary for the optimization of storage, and of overall system design. The measurements include values of wind conditions, temperatures, relative humidity, precipitation, and insolation measured on horizontal surfaces, on vertical surfaces facing in various directions, on a surface facing the sun, and on tilted surfaces facing the equator.

Solar insolation can be measured by means of solar radiometry. The solar radiometry today relies primarily on thermoelectric instruments with electronic read-out and integrating devices to give instantaneous values as well as hourly and daily totals. The basic principles of solar radiometry is discussed in Yellott (1977). A primary objective of solar radiometry is to determine the instantaneous magnitude of direct, diffuse, and total insolation incident upon surfaces which may be tilted at any angle to the horizontal. Solar radiation cannot be measured in transit in the same manner that flowing fluids can be metered with a flow nozzle and a manometer. Instead, it is necessary to intercept a small area of the incoming radiation by a surface which absorbs the radiant energy and convert it into heat. The thermal effect can then be evaluated by calorimetry or by various electrical methods. Silicon photovoltaic cells may also be used, since their short circuit current is a linear function of the incident radiation. Blackened absorbent surfaces are generally insensitive to spectral variations in insolation intensity while photovoltaic cells are spectrally sensitive. Thermal expansion and evaporation of volatile fluids may also be used to produce effects which are proprotional to the incoming solar radiation.

Calculated data of insolation for engineering studies in the utilization of solar energy at the surface of the earth was initiated by Moon (1940), performing through calculations for a standard clear sky, containing reasonable amount of water vapor, of other gaseous atmospheric constituents, and of dust. Moon's spectral curves have been for long a standard in the illumination industry, in the evaluation of selective surface, and in many other solar applications. Moon's clear sky results have been updated by Elterman (1967).

Becker and Boyd (1957) studied the availability of solar energy incident on a surface as affected by the orientation of the surface during cloudless days. Bennet (1966), the U.S. Weather Bureau (1964) and Lof et al. (1966), have prepared maps showing the monthly means of the daily totals of solar radiation (direct plus diffuse radiation incident on a horizontal surface). Farber and Morrison (1975) developed clear - day design values presented in graphical and tabulated form. The calculations performed and the data presented apply to northlatitudes 24 degrees through 64 degrees in 8 degree increments, concerning the irradiation of surfaces inclined at various angles with respect to the horizontal. Daily insolation values on horizontal surfaces can be converted to fairly accurate hourly insolation values on horizontal surfaces with a correlation first made by Whillier (1953), and extended by Liu and Jordan (1960).

2.2.4 Solar Angles and Tilt Angles of Solar Collectors

Due to the changing position of the earth relative to the sun and to the rotation of the earth about its axis, the angle at which the sun's rays reach a surface on the earth changes from day to day and from hour to hour. The sun's position in the sky can be expressed in terms of the solar altitude, β, above the horizontal, and the solar azimuth, ϕ, measured from the south. These angles in turn depend on the local latitude, L; the solar declination, δ, which is a function of the date; and the Apparent Solar Time, expressed as the hour angle, H, where H = 0.25 x (Number of minutes from local solar noon), degree. The following equations relate β and ϕ to the three angles mentioned above:

$$\text{Sin } \beta = \text{Cos } L \ \text{Cos } \delta \ \text{Cos } H + \text{Sin } L \ \text{Sin } \delta \tag{2.1}$$

$$\text{Sin } \phi = \text{Cos } \delta \ \text{Sin } H/\text{Cos } \beta \tag{2.2}$$

Values of β and ϕ for daylight hours of the twenty-first day of each month in 8 degree increments from 0 to 64 degree North latitude can be obtained from ASHRAE Handbook of Fundamentals (1977).

The solar position angles and incident angles for horizontal and vertical surface are shown in Fig. 2.1, where line OQ leads to the sun, the north-south line is SON and the east-west line is EOW. Line OV is perpendicular to the horizontal plane in which the solar azimuth, angle HOS (ϕ), and the surface azimuth, angle POS (Ψ), are located. Angle HOP is the surface-solar azimuth, γ.

The angle of incidence, θ, for any surface is defined as the angle between the incoming solar rays and a line normal to the

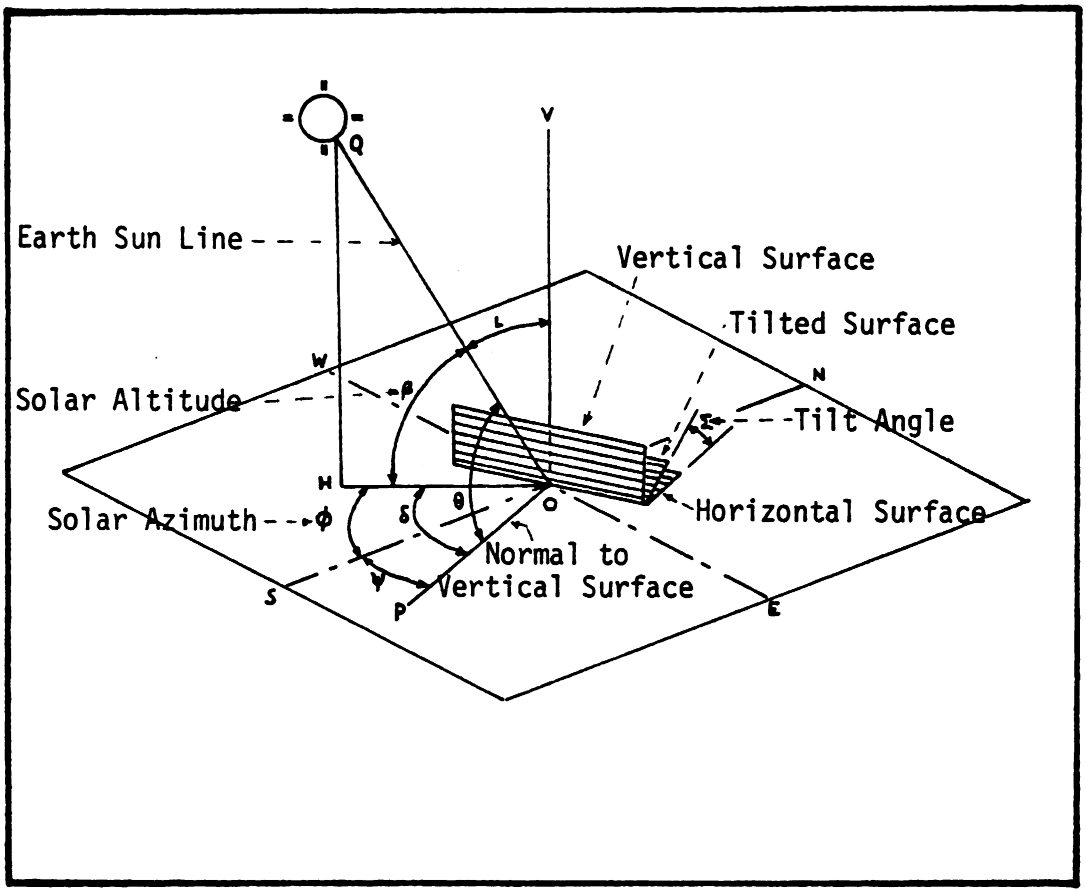

Figure 2.1.--The solar position angles and incident angles for horizontal and vertical surfaces (ASHRAE Handbook of Fundamentals, 1977).

surface. For the horizontal surface in Fig. 2.1, the incident angle θ_H is QOV; for the vertical surface, the incident angle θ_V is QOP. For any surface, the incident angle θ is related to β, γ, and the tilt angle of the surface Σ from the horizontal by:

$$\text{Cos}\ \theta = \text{Cos}\ \beta\ \text{Cos}\ \gamma\ \text{Sin}\ \Sigma + \text{Sin}\ \beta\ \text{Cos}\ \Sigma \qquad (2.3)$$

The optimum tilt angle for a solar collector will depend on the latitude and on seasonal demand based on the uses to which the collected energy is to be put. The daily total radiation incident upon a surface, for all practical purposes, will be a maximum if a south-facing surface is tilted so that the sun's rays are perpendicular to it at solar noon.

2.3 The Flat-plate Solar Collector

There are two types of solar collectors that have been used for many years, i.e., concentrating collectors and flat-plate collectors (Kreider and Kreith, 1975).

Concentrating collectors, the main alternatives to the flat-plate collectors, can only collect direct solar energy and a small fraction of the diffuse solar energy which happens to be at angles close to the sun. The concentrating collectors generally need continuous tracking control, a more expensive mounting structure than the flat-plate collectors, and reflective surfaces which require regular clearing (Kreider and Kreith, 1975).

The flat-plate collector has been the most popular and lowest cost to collect solar heat at modest temperatures. It is also the most frequently considered device for use in the heating and cooling of buildings with solar energy. At temperature below perhaps 140^{o}C there seems to be general agreement that the flat-plate collector is likely to be more economical than concentrating collector (deWinter, 1975).

A typical flat-plate collector consists of one or more transparent flat front plates, one or more insulating zones, bounded by the covers, and an absorbing rear plate (Kreider and Kreith, 1975). Heat is removed from the rear plate by a gaseous or liquid heat transfer fluid, such as air or water. Thermal insulation is usually placed behind the absorber to prevent heat losses from the rear surface. The front covers are generally glass that is transparent to incoming solar radiation and opaque to the infrared reradiation from the absorber. The glass covers act as a convention shield to reduce losses from the absorbing plate beneath. A standard flat-plate collector is shown in Fig. 2.2.

Beside air and water as the working fluid used in solar collectors, hydrocarbon or halogenated hydrocarbons can be used, particularly when power generation or refrigeration is the goal (Edwards, 1977). When heat transfer fluids are rated by technical performance, those with a high thermal conductivity, a low viscosity, and a high specific heat-density product rank high. On this basis air is least desirable, water intermediate, and liquid metal most desirable. Other factors such as a low freezing point, non-corrosiveness, safety of life and property, and low cost overturn a simplictic ranking on the basis of heat transfer performance. When warm air is the desired goal as for drying or space conditioning, the

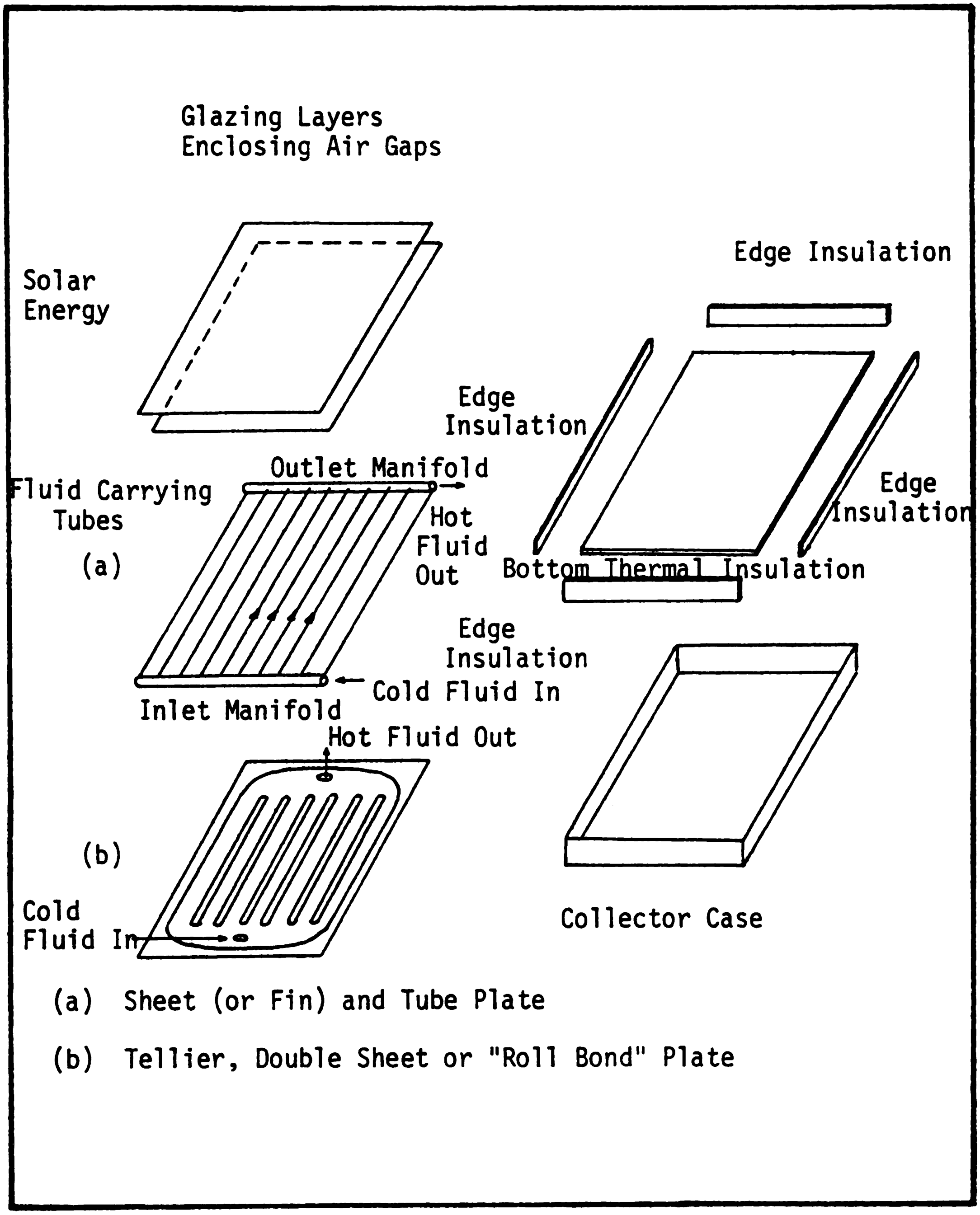

Figure 2.2.--Standard flat-plate collector.

non-corrosive nature of air has the advantage of being safe for use as the heat carrying medium and relatively costless.

For water systems the abosrbing plate can be any metal, plastic, or rubber sheet that incorporates water channels, while for air systems the space above the absorbing plate can also serve as the conduit. Many metal products, such as the aluminum, copper, and steel are suitable for use as absorbers in water or air systems (Edwards, 1977).

The amount of solar energy collected is governed by: a) the transmittance of the transparent covers, b) the absorptance of the absorbing plate to the incident radiation, c) thermal resistance between the absorber surface and the heat transfer fluid, and d) emittance of the absorber plate surface in the infrared spectrum (Kreider and Kreith, 1975). In general, the thermal conversion performance of solar collectors can be improved by increasing the transmission of energy through the collector to the working fluid and by reducing thermal losses.

The absorptance of the absorbing plate should exceed a level of 95 percent. This level can be obtained by means of appropriate coating. The surface of the absorbing plate may be a flat black paint with an appropriate primer. The primer coat should preferably be thin since a thick undercoat of paint would increase the resistance of heat transfer. The primer should be of the self-etching type. If the primer is not a self-etching type, the repeated thermal expansion and contraction of the plate may cause the paint to peel after a year or so (Kreider and Kreith, 1975).

Brooks (1936) used the concept of selective surfaces in flat-plate collectors and developed extensive tables of the absorptivity and emissivity of surfaces, and a discussion of their significance. Tabor (1955 a, b, c) revived interest in the use of selective surfaces in flat-plate collectors. Since then Tabor had conducted many experiments on selective surfaces. The use of a selective surface in an experimental collector led Tabor (1958) to a revision of the convection and radiation heat loss equations originally proposed by Hottel and Woertz (1942). The original equations had proved adequate for gray surfaces but led to excessively low heat loss predictions in collectors featuring selective coatings.

The selective surface with the best radiation properties to date is probably "nickle black" or "chrome black", both of these were first developed by Tabor (1962 and 1963). Other selective surfaces include silver oxide on silver, dielectric interference layers on aluminum, copper oxide on aluminum, iron oxide on steel, and copper oxide on copper and other metals. Only the nickle black and copper oxide coatings are at present used in practice (Tabor, 1977).

III. MATHEMATICAL RELATIONSHIPS OF COLLECTOR PERFORMANCE

3.1 The Solar Collector as Heat Exchanger

Basically a flat-plate solar collector works as a heat exchanger. The heat absorbed from the sun by the absorbing plate is transferred to either air or water as the heat transfer fluid. The amount of heat obtained for air medium collectors is partially governed by the convection heat transfer coefficient between the absorbing plate and either the laminar or turbulent air flow.

Heat transfer coefficients for common surface geometries are given in many heat transfer textbooks. The convective heat transfer coefficient can be expressed as a function of the dimensionless group called the Nusselt number (Nu):

$$h_c = Nu \frac{k}{L} \qquad (3.1)$$

where h_c = convective heat transfer coefficient, $W/m^2.{}^oC$

Nu = Nusselt number, dimensionless

k = thermal conductivity, $W/m.{}^oC$

L = length, m

For fully developed turbulent flow of gases inside tubes, Kays (1966) recommends

$$Nu = 0.022\ Re^{0.8}\ Pr^{0.6} \qquad (3.2)$$

where Nu = Nusselt number, dimensionless

Re = Reynolds number, dimensionless

Pr = Prandtl number, dimensionless

and for liquids with a Prandtl number between 1.0 and 20

$$Nu = 0.0155\ Re^{0.83}\ Pr^{0.5} \tag{3.3}$$

For laminar flow inside tubes, Kreith (1973) gives the following equation which is useful in solar systems, since the pipes are often short and fully developed turbulent conditions may not exist:

$$Nu = \frac{Re\ Pr\ D}{4L}\ \ln\left[1 - \frac{2.654}{Pr^{0.167}\ (Re\ Pr\ D/L)^{0.5}}\right]^{-1} \tag{3.4}$$

where Nu = Nusselt number, dimensionless

Re = Reynolds number, dimensionless

Pr = Prandtl number, dimensionless

D = diameter, m

L = length, m

This equation is valid for flow in tubes when L/D is less than 0.0048 Re, and in flat ducts when L/D is less than 0.0021 Re.

Most of the flat plate solar collectors with air as the heat transfer fluid have flat rectangular ducts. Only one side of the air duct, i.e., the absorbing plate, is heated. For an active solar collector, the forced convection may develop a turbulent flow inside the duct. The following correlation for fully developed turbulent flow between flat plates with one plate heated can be derived from Kays' data:

$$Nu = 0.0158\ Re^{0.8} \tag{3.5}$$

Whenever the flow/length ratio to hydraulic diameter is in the order of ten or less, consideration should be given to the development of the boundary layers which may cause an increase in the Nusselt number. Tan and Charters (1970) experimentally studied the flow of air between parallel plates with small aspect ratios for use in solar air collectors. Their results showed higher heat transfer coefficients by about 10 percent as compared to those by Kays in which an infinite aspect ratio was used.

The quantity of heat absorbed by the air from the plate depends upon the design of the total heat removal system of the collector. It is not possible to transfer all of absorbing plate heat to the air. Some of the plate heat is lost to the lower temperature surrounding the collector and ambient conditions. Heat losses occur upward through the transparent cover plate, downwards through the back insulation, and sideways through the edge insulation.

The performance efficiency of a solar collector can be described by an energy balance that accounts for the distribution of incident solar energy into useful energy gain and the various losses. Duffie and Beckman (1974) presented the energy balance of a collector as:

Rate of incident energy absorbed = rate of useful heat transfer to a working fluid in the solar exchanger

+ rate of energy losses from the collector to the surroundings by re-radiation, convection, and conduction

+ rate of energy storage
in the collector.

(3.6)

The factors influencing the collector performance are discussed in the following sections.

3.2 Thermal Losses from the Collector

The critical factors that affect the upward heat transfer are temperature of the absorbing plate, temperature of the ambient air, temperature of the surroundings, the number of transparent cover plates and their spacing, angle of tilt of the collector from the horizontal, wind speed over the cover plate, and the transmittance of the cover material (Whillier, 1977).

The upward heat loss coefficient of the collector, U_{up}, was defined by the relation (Whillier, 1977):

$$q_{up} = U_{up} (t_c - t_a) \quad (3.7)$$

where q_{up} = upward heat transfer rate through the transparent cover, W/m^2

U_{up} = upward heat loss coefficient of the collector, $W/m^2.{}^oC$

t_c = absorbing plate average temperature, ^oC

t_a = ambient air temperature, ^oC

Equations have been derived by Hottel and Woertz (1942) and Whillier (1964) for calculating U_{up} for various combinations of glass and plastic in the cover system. For a collector with one transparent cover, the equation is:

$$U_{up} = \tau\varepsilon_c h_{r_{cs}} \left[\frac{t_c - t_s}{t_c - t_a}\right] + \frac{1}{\dfrac{1}{h_{c1} + E_{c1} + h_{r_{c1}}} + \dfrac{1}{h_w + \varepsilon h_{r_{1s}}\left(\dfrac{t_1 - t_s}{t_1 - t_a}\right)}} \qquad (3.8)$$

where U_{up} = upward heat loss coefficient of the collector, $W/m^2.^oC$

τ = transmittance of the cover material for long-wave radiation, decimal

ε_c = emissivity of the absorbing plate, decimal

ε = emissivity of the cover material, decimal

E_{c1} = emissivity factor, decimal

$h_{r_{cs}}$ = equivalent radiative coefficient, $W/m^2.^oC$

h_{c1} = convection coefficient, $W/m^2.^oC$

h_w = wind coefficient, $W/m^2.^oC$

t_c = absorbing plate average temperature, ^oC

t_s = equivalent black body temperature of the sky, ^oC

t_a = ambient air temperature, ^oC

t_1 = transparent cover temperature, ^oC

Equation (3.8) includes wind coefficient, convection coefficient, equivalent radiative coefficient, and emissivity factor.

The wind coefficient can be calculated using a dimensional expression given by McAdams (1954) which relates the heat transfer coefficient in $W/m^2.^oC$ to the wind speed in m/s:

$$h_w = 5.7 + 3.8\ V \qquad (3.9)$$

Convection coefficient, equivalent radiative coefficient, and emissivity factor can be calculated using the following equations (Whillier, 1977):

$$h_{xy} = C\ (t_x - t_y)^{\frac{1}{4}} \qquad (3.10)$$

$$h_{r_{xy}} = \sigma\ (T_x^4 - T_y^4)/(t_x - t_y) \qquad (3.11)$$

$$E_{xy} = \frac{1}{\frac{1}{\varepsilon_x} + \frac{1}{\varepsilon_y} - 1} \qquad (3.12)$$

Various values of the constant C in Equation (3.10) are 0.24, 0.21, 0.18, and 0.15 for tilt angles of 0^o, 30^o, 60^o, and 90^o respectively.

The downward or back heat loss coefficient, U_b, depends on the heat resistance values of the materials used for insulation beneath the absorbing plate and or the air channel. The thickness of the insulation depends on the position of the collector. If the back of the solar collector does not rest firmly on a roof or is not protected in any other way from the wind, greater losses should be expected. Sufficient insulation should be provided to keep U_b less than one tenth of U_{up} (Whillier, 1977).

The edge heat loss can be important in small collectors where the perimeter - to - collector area is relatively large (0.375 or more). The recommended minimum thickness of edge insulation is 25 mm with heat loss coefficient of 0.25 $W/m^2.^oC$, and generally it should be at least half the thickness of the back insulation, depending upon the degree of exposure of the edges (Whillier, 1977). The calculation of the edge heat losses is a complex process because of the complicated geometry involved. It has been done by Tabor (1955). For a typical edge insulation with 10 mm wide gap between the absorbing plate and the edge wall, the edge heat loss coefficient would be about 0.45 $W/m^2 \cdot {}^oC$, i.e.,

$$q_{edge} = 0.45\ (D)\ (P)\ (t_c - t_a) \tag{3.13}$$

where q_{edge} = heat loss rate through the edge, W/m^2

D = depth of the collector, m

P = perimeter, m

t_c = absorbing plate average temperature, ^oC

t_a = ambient air temperature, ^oC

The overall collector heat loss coefficient, U_L, can be presented as follows:

$$U_L = U_{up} + U_b + U_{edge} \left(\frac{A_p}{A_c} \right) \tag{3.14}$$

where A_p = perimeter area of the collector, m^2

A_c = collector area, m^2

And the heat loss rate from the collector is

$$q_L = U_L\ (t_c - t_a) \tag{3.15}$$

3.3 The Heat Collection

The quantity of useful heat collection is governed by various factors, some of which have been discussed in the preceeding sections. An equation for calculating the useful heat obtained from a conventionally designed solar collector has been derived by Whillier (1964).

The following heat transfer analysis has been based on Whillier's work in order to clarify the factors that govern the performance of solar air collector. Fig. 3.1 shows a section of a solar collector of conventional design, of width B and length L, with the air flowing behind the absorber plate.

At a distance x from the inlet end, the temperature of the air being heated is t. The temperatures of other surfaces at this position are as shown in Fig. 3.1; t_c is the temperature of the plate that absorbs the solar radiation, and t_r is the temperature of the back surface. The ambient air temperature is t_a. It was assumed that there was no downward heat loss through the back insulation.

The performance of the solar collector was expressed in terms of two temperatures; namely, the ambient temperature, t_a, and the temperature t_1, at which the air enters the collector. Heat balances on the absorbing plate and on the rear plate are set up to eliminate the temperatures t_c and t_r. The heat balances are:

Heat balance for the absorbing plate:

Solar radiation absorbed by element of plate of width B, length x	=	Heat loss upward from absorbing plate through transparent over	+	Heat flow into air stream by conduction	+	Heat radiated downwards from absorbing plate to the back plate

$$Hf\ (B\ \delta\ x) = U_L\ (B\ \delta\ x)\ (t_c - t_a)\ + h_c\ (B\ \delta\ x) + h_rE\ (B\ \delta\ x)\ (t_c - t_r) \quad (3.16)$$

Heat balance for the back plate:

Net radiation received from absorbing plate	=	Heat flow into air stream from the back plate by convection

$$h_rE\ (B\ \delta\ x)\ (t_c - t_r) = h_c\ (B\ \delta\ x)\ (t_r - t) \quad (3.17)$$

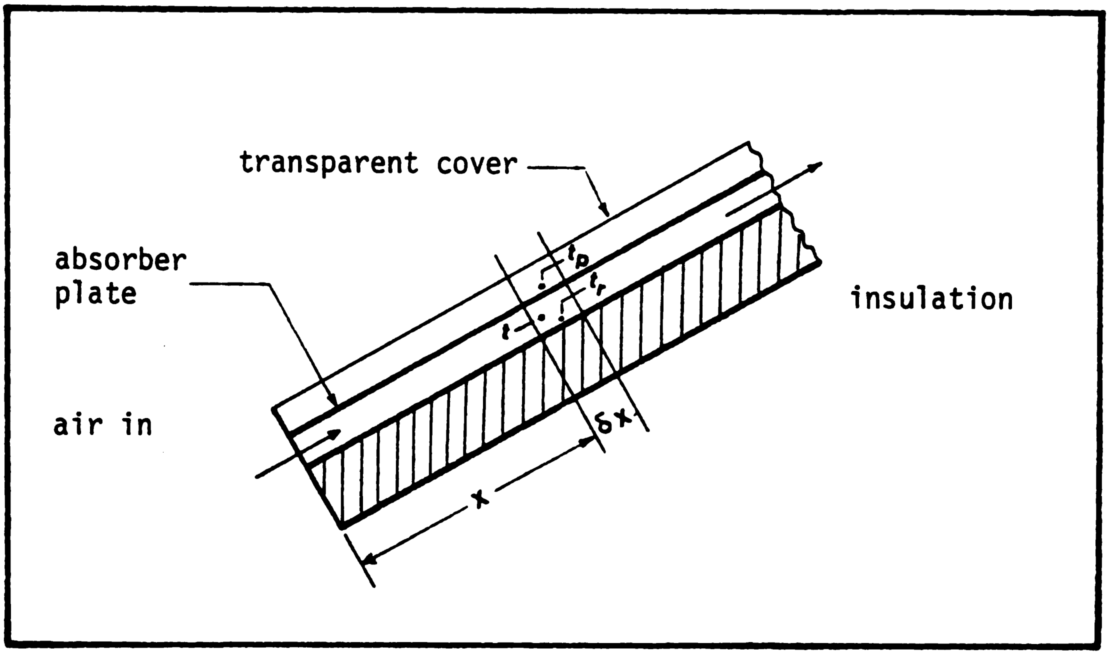

Figure 3.1.--A section of a conventional air solar collector.

Heat balance for the back plate:

Net radiation received from absorbing plate	=	Heat flow into air stream from the back plate by convection

$$h_r E\ (B\ \delta\ x)\ (t_c - t_r) = h_c\ (B\ \delta\ x)\ (t_r - t) \tag{3.17}$$

Heat balance on element of air stream:

Enthalpy rise of air stream in passing through element of length x	=	Heat flow into air stream downward from absorbing plate	=	Heat flow into air stream upward from back plate

$$WC_p \frac{dt}{dx}\ \delta\ x = h_c\ (B\ \delta\ x)(t_c - t) + h_c'\ (B\ \delta\ x)(t_r - t) \tag{3.18}$$

Integration over the length of the collector leads to an equation giving the useful heat collected in terms of the heater design parameter and the incident solar energy. Equation (3.16) and Equation (3.17) were used to eliminate the unknown temperatures t_c and t_r from Equation (3.18). Thus:

$$\frac{WC_p}{B}\ \frac{dt}{dx} = \frac{1}{1 + U_L/h} \left[Hf - U_L(t - t_a) \right] \tag{3.19}$$

The term $1/(1 + U_L/h)$ is known as the efficiency factor, F'. The solution of Equation (3.19) with boundary condition of x = 0, and an inlet temperature of t_1, gives

$$\frac{t - t_a - Hf/U_L}{t_1 - t_a - Hf/U_L} = \exp\left[- \frac{BF'U_L x}{WC_p} \right] \tag{3.20}$$

At the exit end of the air collector, i.e., at x = L, the air temperature is t_2, and the temperature rise through the air collector is $(t_2 - t_1)$, given by

$$(t_2 - t_1) = (Hf/U_L - (t_1 - t_a)\ (1 - \exp\left[- \frac{F'U_L}{GC_p} \right]) \tag{3.21}$$

where G = W/BL is the mass flow rate of air per unit collector area.

The overall coefficient of heat transfer from the air inside the collector to the ambient air is

$$U_o = 1/(\frac{1}{U_L} + \frac{1}{h}) \qquad (3.22)$$

so that

$$F' = \frac{U_o}{U_L} \qquad (3.23)$$

The term $F'U_L/GC_p = U_o/GC_p$ is identical to the number of transfer unit or NTU, that is of such common occurence in heat exchanger theory.

Multiplying the temperature rise $(t_2 - t_1)$ by the flow rate per unit area, Equation (3.21) to obtain the desired expression for the rate of useful heat collection per unit area of the collector:

$$q_u/A = GC_p\ (t_2 - t_1) \qquad (3.24)$$

or

$$q\ /A = (\frac{1}{1 + U_L/h})\ (\frac{1 - e^{-U_o/GC_p}}{U_o/GC_p})\ (Hf - U_L(t_1 - t_a)) \qquad (3.25)$$

The term $(1 - e^{-U_o/GC_p})/U_o/GC_p)$ is known as the flow factor, F". Factor f is the effective transmissivity - absorptivity product of the collector cover system. Equation (3.25) can be rewritten as

$$q_u/A = F'\ F''\ (Hf - U_L\ (t_1 - t_a)) \qquad (3.26)$$

The product F' F" is sometimes referred to as the heat removal factor and that its value is equal to the ratio of the log mean temperature difference to the inlet temperature difference.

Equation (3.26) shows that the inlet temperature is different (usually higher) than the ambient air temperature. This occurs in solar air collectors with closed systems which recycle the air through the collector.

For an open system in which the inlet temperature is the ambient air temperature (no recycling), it is convenient to use Equation (3.24) for calculating the actual useful heat collection. In terms of enthalpy of the inlet and outlet air, Equation (3.24) can be written as

$$q_u/A = \frac{G\ (EN2 - EN1)}{3.6} \qquad (3.27)$$

where q_u/A = actual useful heat collection, W/m^2

G = air mass flow rate, $kg/hr/m^2$

EN1 = enthalpy of the inlet air, kJ/kg

EN2 = enthalpy of the outlet air, kJ/kg

3.4 The Collector Efficiency

The solar air collector efficiency can be defined as the ratio of the actual useful heat collected to the solar energy incident upon or intercepted by the collector (Kreider and Kreith, 1975). In equation form the solar air collector efficiency can be written as

$$\eta = \frac{q_u/A}{H} = \frac{GC_p\ (t_2 - t_1)}{H} \qquad (3.28)$$

Equation (3.28) is used to determine the instantaneous efficiency of the collector with open system. When using the instantaneous method, the measurement of parameters includes the mass flow rate of the air, the difference in air temperature between the inlet and outlet, and the solar insolation. This is done simultaneously and under steady state conditions.

The collector efficiency with closed system is usually evaluated using calorimetric procedure (Hill and Elmer, 1977). The efficiency can be expressed as

$$\eta = \frac{q_u/A}{H} = f - U_L \frac{(t_c - t_a)}{H} \tag{3.29}$$

or

$$\eta = F'f - F'U_L \frac{\frac{t_1 + t_2}{2} - t_a}{H} \tag{3.30}$$

or

$$\eta = F_R f - F_R U_L \frac{(t_1 - t_a)}{H} \tag{3.31}$$

where F_R is the product F" F' frequently referred to as the collector heat removal factor and H is the insolation rate.

Equation (3.29), (3.30), and (3.31) indicate that if the efficiency is plotted against some appropriate Δt/H, a straight line will result where the slope is U_L and the Y intercept is f.

IV. MATERIAL AND METHOD OF STUDY

4.1 Material of Study

The solar collector studied in this experiment was a flat-plate, single air-pass collector. The collector was designed and constructed primarily to provide supplemental heat for a 5,000 laying hen cage-type poultry house and secondarily for drying poultry excreta. This type of collector is relatively low in cost and easy to construct. The material used were ordinary farm building materials such as lumber, poles, plywood, glass, black painted aluminum roofing, and insulation materials. This was done to minimize material costs (approximately $2.63 per square foot of collector surface area in 1976) and provide a collector system that can be constructed by farm building contractors or farmers.

The collector was constructed separately from the poultry house as the building already existed but was not oriented properly. The collector was located on the north side of the house rather than the south for operational and management convenience of the project. A schematic plan of the house and the collector is shown in Fig. 4.1. The collector was positioned at a 60^{o} tilt angle from the horizontal and facing south. This meets the rule-of-thumb guideline for optimizing winter solar radiation in the northern hemisphere by being constructed at an angle equal to the latitude of East Lansing area

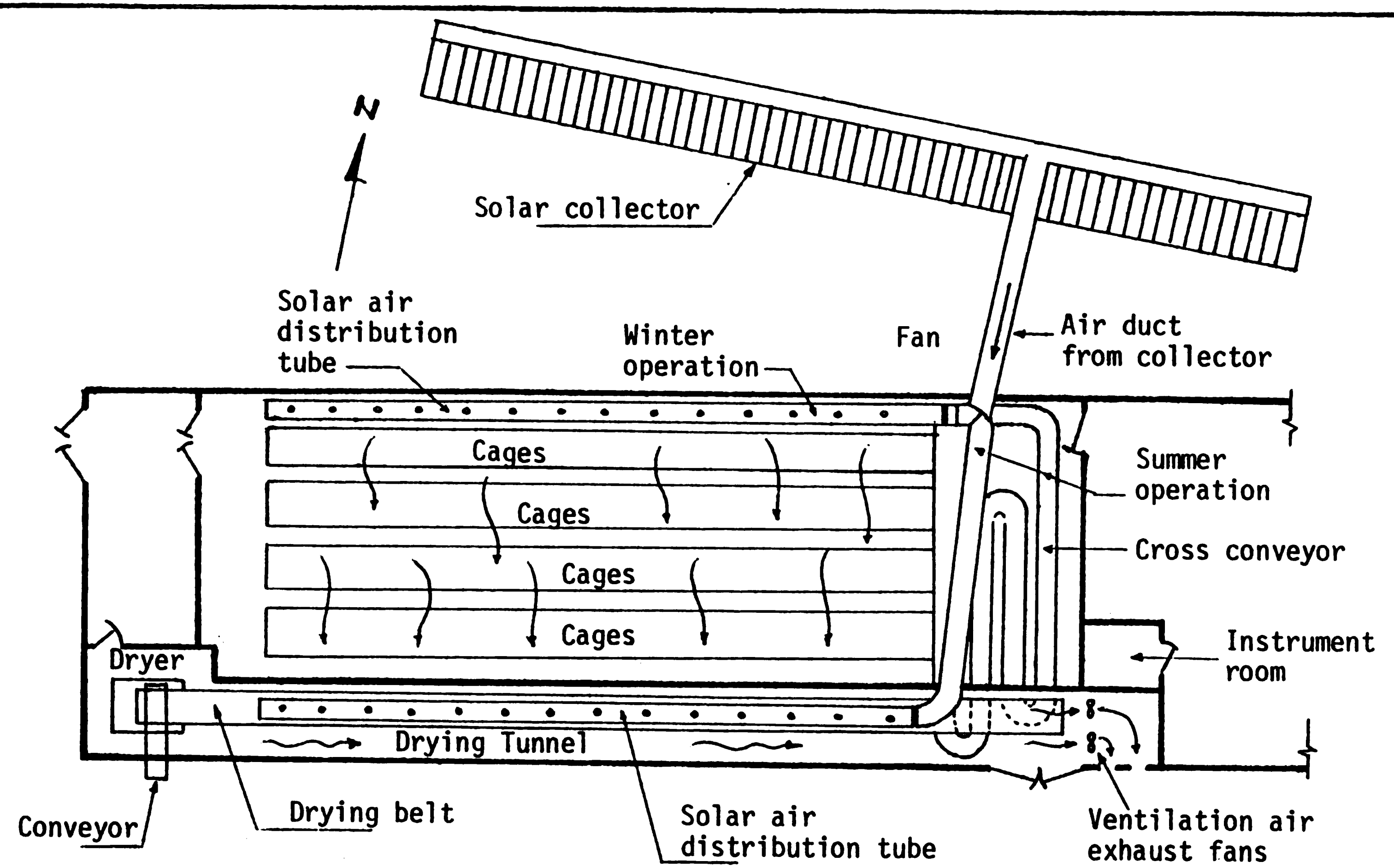

Figure 4.1.--A schematic plan of a 5,000 bird laying house with a solar collector for supplemental heating and excreta drying.

(45°) plus 15°. However, this collector was also used for various year round operations.

The gross area of the collector was 93.4 m^2 with 46 mm by 305 mm panels. The whole structure was 3.05 m wide and 30.62 m long. Square ridged, black painted aluminum roofing material was used as the absorbing plate, covered with a single glazing of 3.18 mm tempered glass supported 19.1 mm above the absorbing plate. The corrugated aluminum sheet is a common farm building structural material and also meets the requirements for being thin and a good conductor. The solar shortwave radiation is absorbed by the black surface, but due to the thinness and high conductivity of the aluminum sheet the under-surface is essentially the same temperature as the black top surface. The glass was separated by approximately 25.4 mm dead air space from the absorbing plate to minimize loss of heat back through the glass to the outside lower ambient temperature. The air duct behind the absorbing plate was 57 mm by 457 mm wide. The moving air through this duct was heated as it moved adjacent to the under surface of the aluminum sheet. The details of the collector are shown in Fig. 4.2 and Fig. 4.3.

A 432 mm duct was placed along the top of the collector and a 610 mm main duct ran from the center point of the collector to the poultry house. Approximately 184 mm of fiber glass blanket insulation was used to insulate the back of the collector and the ducts. The oustide of the dust insulation was covered by

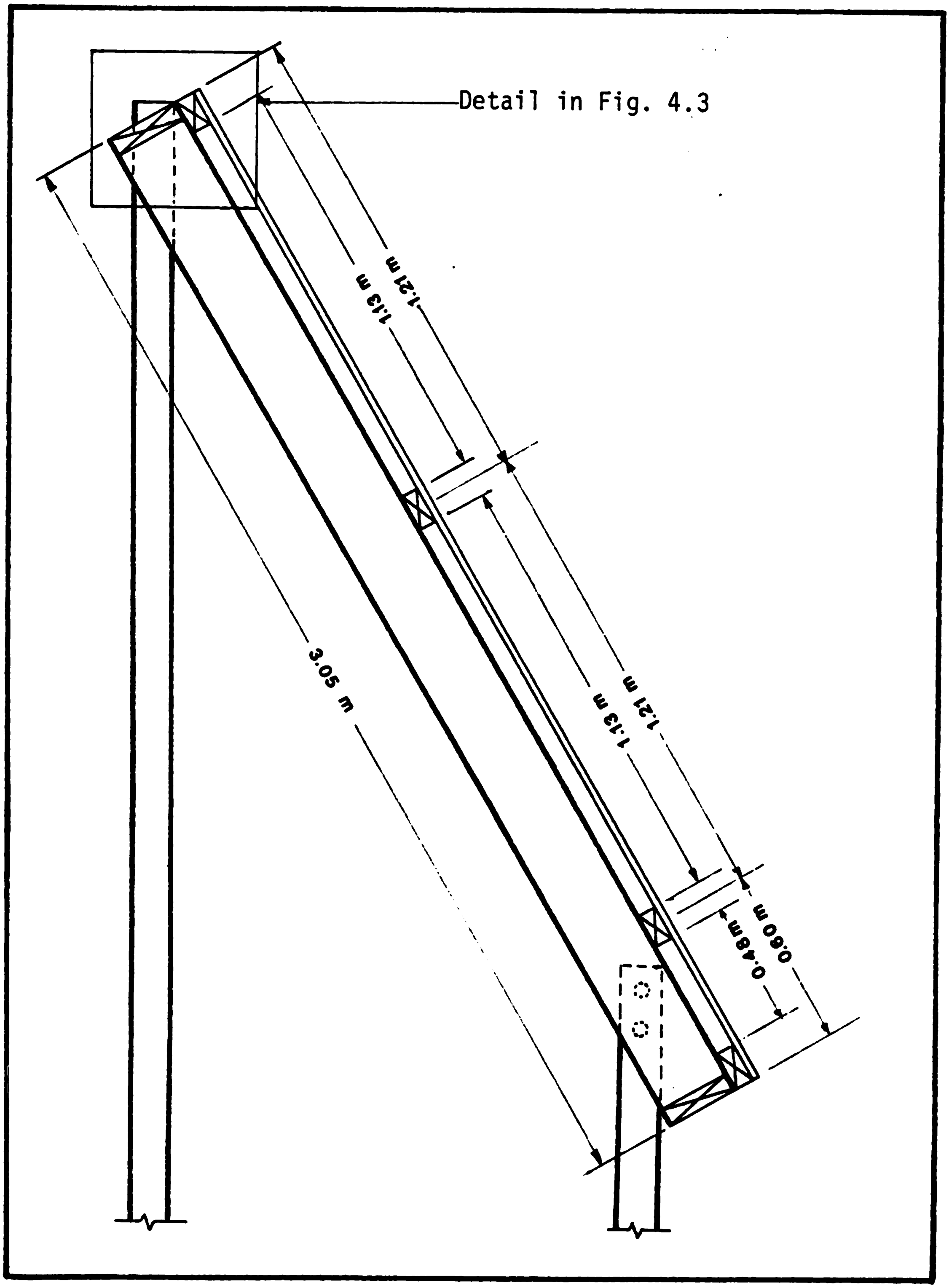

Figure 4.2.--Flat-plate, single air pass collector (side view)

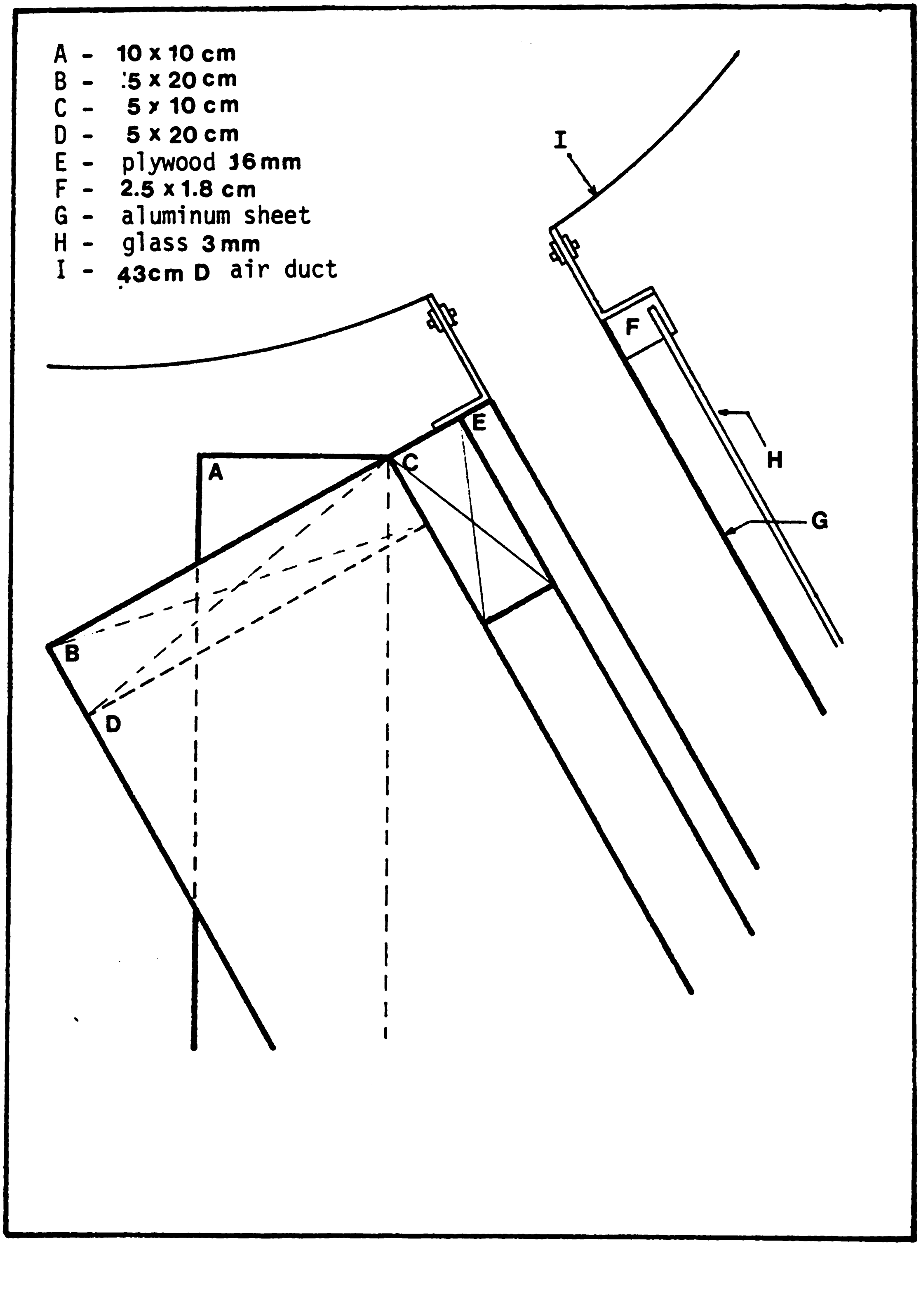

Figure 4.3.--Detail of Figure 4.2

black polyethelene plastic. Due to the position of the collector, a small area of the collector surface was shadowed by the main duct during operation. The effective or net area of the collector surface was approximately 90.6 m^2.

The total air flow from the collector was controlled with a fan mounted in the main collector duct just inside the poultry house. The variable speed fan used had an output range up to 141.58 m^3/minute (5,000 cfm).

4.2 Method of Study

Three different air-flow rates of 0.32, 0.48, and 0.64 m^3/min./m^2 were used in this experiment to determine the effect of the air-flow rate on the collector efficiency. These air-flow rates were in terms of volumetric air flow per unit area of the absorbing plate. The collector was operated experimentally during the clear days during the spring and early summer of 1978.

The efficiency of the collector is defined as the ratio of the actual useful energy collected to the solar energy incident upon or intercepted by the collector. The SI unit system was used in the analysis of the data. Energy was calculated in unit energy per unit of collector area per unit of time (kJ/m^2/hr.).

The data required for analysis in this research consisted of:

a) inlet or outside ambient temperature, ^oC

b) outside relative humidity, percent

c) outlet air temperature from the collector, ^oC

d) absorbing plate temperature, ^oC

e) wind speeds, m/s

f) wind direction

g) incident solar radiation, $kJ/m^2/hr$.

The data were recorded simultaneously in 30 minute intervals from 8:00 a.m. through 6:00 p.m. using Digital Data Acquisition System (DDAS). Any physical effect capable of translation into a DC voltage may be recorded with a DDAS.

The collector used in this experiment was an open system type. The heat collected was calculated using the following equation (from Equation 3.25):

$$q_u/A = G\ (EN2 - EN1) \qquad (4.1)$$

where q_u/A = actual useful heat collected, $kJ/M^2/hr$.

G = mass-flow rate of air per unit collector area, $Kg/hr./m^2$

EN1 = enthalpy of the inlet air, kJ/Kg of dry air

EN2 = enthalpy of the outlet air, kJ/Kg of dry air

The outside ambient air temperatures, the outlet air temperatures from the collector, and the outside relative humidities were the parameters used to compute the enthalpies. The SI psychart computer program developed by Bakker-Arkema, Brook, and Lerew (in Pomeranz, 1978) was used for the computations.

The instantaneous efficiency of the collector was calculated using the following equation (from Equation 3.26):

$$\eta = \frac{q_u/A}{H} \qquad (4.2)$$

where η = instantaneous efficiency of the collector, precent

q_u/A = actual useful heat collected, $kJ/m^2/hr$.

H = incident solar radiation, $kJ/m^2/hr$.

4.3 Measurements and Instrumentation

The measurements of the air flow through the main collector duct and other parameters required were carried out with the following instruments or devices:

a) AEI velometer

b) Copper-constantan thermocouples

c) relative humidity (RH) and temperature sensor

d) wind sensor for speed and direction

e) sol-a-meter or pyranometer

f) DDAS recorder

The copper-constantan thermocouples, RH and temperature sensor and transmitter unit, wind sensor unit, and sol-a-meter were connected to the DDAS recorder that can provide various data in millivolt outputs simultaneously in a certain time interval. The recorder was set to record data at 30 minute intervals.

4.3.1 Air flow Measurement

Three different air-flow rates of 0.32, 0.48, and 0.64 m^3/min./m^2 were obtained during the operations of the collector by adjusting the fan speed. An AEI velometer was used to check the air velocity through the main collector duct. The mean air velocity through the duct was determined by measuring the air velocities at five locations in equal concentric areas across the duct. The arrangement of these five locations are shown in Fig. 4.4.

The following equation was used to determine the air-flow rate:

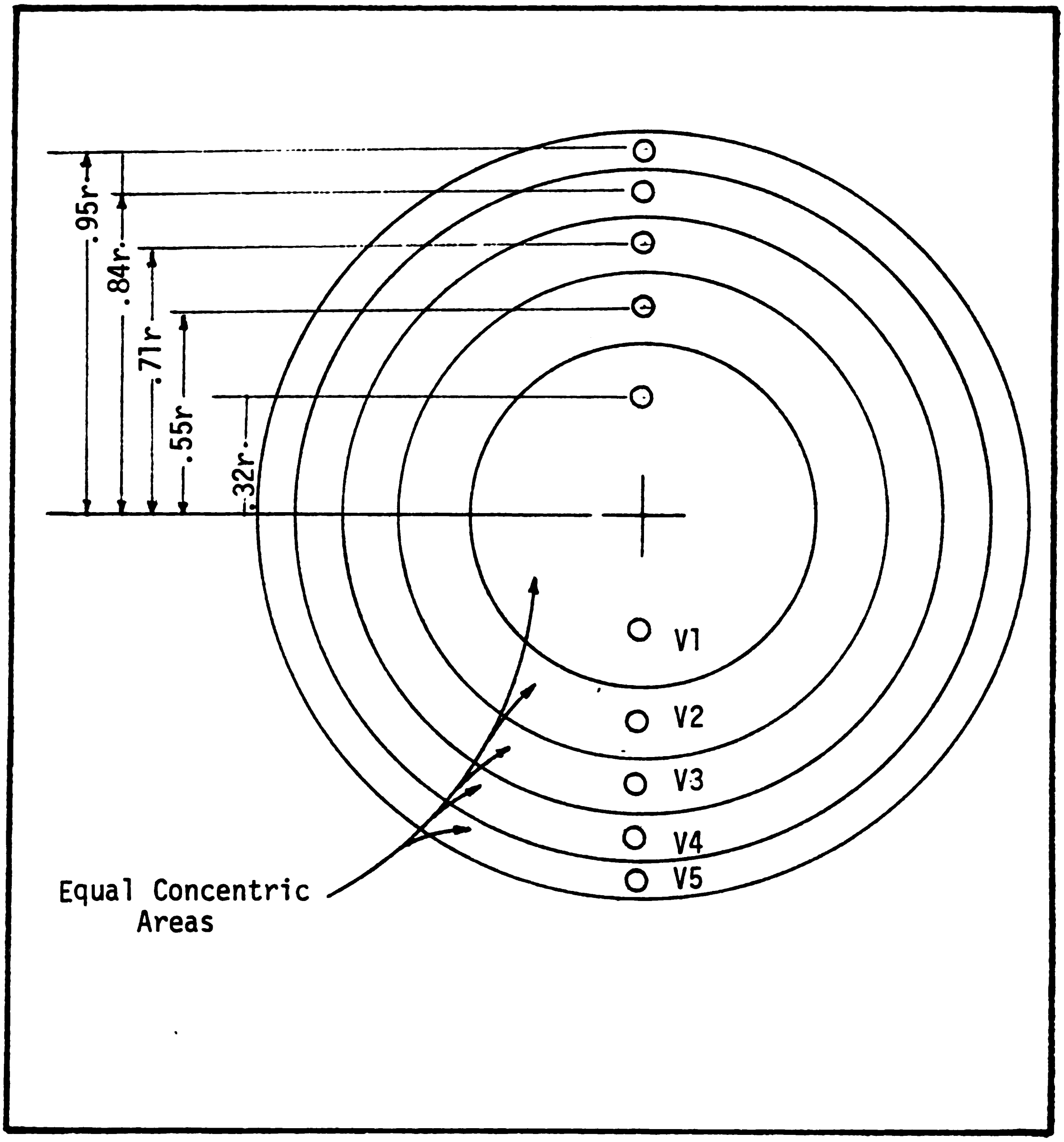

Figure 4.4.--Five locations of velocities measurement in equal concentric areas.

$$q = \frac{(V1 + V2 + V3 + V4 + V5) \quad r^2}{5} \tag{4.3}$$

where q = air flow rate, m^3/min.

V1..V5 = air velocities, m/min.

r = radius of the duct, m.

The air-flow rates were checked to insure the stability of the air flow during each operation of the collector.

4.3.2 Temperatures Measurements

Copper-constantan thermocouples were used to sense the temperature at various desired locations. Thermocouples were attached behind the absorbing plate in the air stream, to the absorbing plate, and in the main collector duct.

The millivolt outputs were converted to temperature values using the empirical relation (Lamoureux, 1975):

$$t = a_0 + a_1V + a_2V^2 + a_3V^3 + \ldots\ldots \tag{4.4}$$

where t = temperature, ^oC

V = electromotive force (emf) outputs of the thermocouples, mV

a_i = coefficients

The coefficients used in the above equation to convert millivolts to degrees centigrade with a 0^oC reference junction are presented in Table 4.1

The copper-constantan thermocouples are capable of measuring temperatures ranging from -200 to 400^oC with standard error of 0.425^oC.

TABLE 4.1.--Coefficients for conversion of copper-constantan thermocouple readings.

Coefficients	Values
a_0	- 0.101163
a_1	25.5932
a_2	- 0.695815
a_3	0.0799528
a_4	- 0.0123173
a_5	0.00107824
a_6	$- 4.96382 \times 10^{-5}$
a_7	6.95069×10^{-7}

Source: R. T. Lamoureux (1975). Instruments and Control Systems.

4.3.3 Relative Humidity and Temperature Sensor

The outside relative humidities and outside ambient temperatures were measured with a RH and temperature sensor instead of using thermocouples (for measuring dry bulb and wet bulb temperatures). The use of wet bulb thermocouples presents the problem of freezing temperatures during winter time.

A General Eastern Model 411 RH and temperature sensor and a Model 450 RH and temperature transmitter were used to measure the outside relative humidities and ambient air temperatures directly. The Model 450 RH and temperature linearization and amplification module is intended as a companion electronics unit providing signal conditioning for the Model 411 RH and temperature sensor. This model utilizes solid state circuitry and provides dual, linear 0 - 5 vdc low impedance outputs for 0 - 100% RH and -50 to 50^{o}C temperature spans.

This RH and temperature sensor and transmitter require an adapter box before connected to a DDAS recorder to adjust the outputs in millivolts.

4.3.4 Wind Speed and Direction Measurement

A Weathertronics Stratvane wind sensor Model 2111 was used to measure wind speed and direction. This model is an industrial grade combination of anemometer and wind vane, constructed of corrosive resistant materials and be able to withstand wind speed of approximately 320 Km per hour (200 mph). Starting threshold for the vane is approximately 1 m/s. The Stratavane is supplied with a selsyn motor for wind direction. The accuracy of speed and direction measurements are ± 0.01 and 3^{o}, respectively.

A signal conditioning or translator is needed in conjunction with data acquisition system. Weathertronics translator Model 2210 was used for this purpose. This translator features three aluminum extruded boxes with a common modular power supply. The standard translator includes a wind direction and a wind speed signal conditioning module. Each signal conditioning module has a reference voltage for sensor excitation.

4.3.5 Insolation Measurement

A silicon photovoltaic cell pyranometer was used to measure the solar radiation incident upon the surface of the collector. At constant temperature, the short circuit current of silicon cell is a linear function of the incident solar radiation intensity. The current from a single 2 cm^2 cell under full terrestrial sunshine (1,000 W/m^2 or 318 Btu/hr./$ft.^2$) could readily exceed 100 milliampres. A 100 millivolt signal results when the cell is short-circuited by a 1.0 ohm resistance. The temperature sensitivity of the cell is minimal. The use of a low resistance with a negative temperature characteristic in thermal but not electrical contact with cell virtually eliminates variation of cell output with changes in ambient temperature within the range encountered in actual practice.

The silicon photovoltaic cell pyranometer used in this measurement was Matrix MK I-G sol-a-meter. This standard instrument was designed to operate with 0 - 10 mV or 0 - 100 mV recorders. This instrument was calibrated for insolation values of 0 - 2 cal/ cm^2/min.

The following equation was used to convert the millivolt outputs to energy in cal/cm^2/min. using calibration factors:

$$mV \times 0.0163 + 0.078 + cal/cm^2/min. \qquad (4.5)$$

This instrument was set up at the same tilt angle as the collector (60^o from the horizontal plane) so that the efficiency of the collector could be calculated directly. The tilt angle had no effect on the cell performance.

4.3.6 Digital Data Acquisition System Recorder

The copper-constantan thermocouples, RH and temperature sensor and transmitter unit, wind sensor unit, and pyranometer were connected to a digital data acquisition system recorder. An Esterline-Angus Model D-2020 was used for this purpose. This type of instrument is a digital DC-millivolt measuring device that provides a visual digital display and a digital printed output of the measured values up to 20 analog input signals. In addition, the unit also incorporates a real time, solid state, 24 hour digital clock, the time of which can be both visually displayed and printed out.

The insolation data were measured in cumulative values for 30 minute intervals. This could be provided by incorporating an integrator unit. The use of an integrator unit with the Model D-2020 recorder provided a means of recording values that represent the time integration of a variety of analog input values, rather than the instantaneous values as normally recorded by the Model D-2020. The digitized data recorded for each integrated analog channel is a totalization of virtually all input values over a selected period of time.

V. RESULTS AND DISCUSSION

The raw data of this experiment consisted of inlet or ambient air temperatures, outlet air temperatures, outside relative humidity levels, and insolation magnitudes. The SI-psychart computer program was used to compute the data for desired analysis of performance of the collector. The weather conditions in Michigan during the Spring of 1978 were mostly cloudy. Due to the cloudiness, only 15 fairly clear days could be used for data analysis. Some additional data were obtained from the following summer operation. The data are tabulated and presented in the appendix.

5.1 Effect of Air-flow Rate on the Collector Efficiency

The effect of air-flow rate on the thermal efficiency of the solar collector was calculated for a daily average and at 13:00 hours. The results are tabulated in Table 5.1 and Table 5.2. The relationship between the volumetric air flow rate and the instantaneous efficiency of the collector was analyzed using simple linear regression. Figure 5.1 and Figure 5.2 present the results of these two analyses. It will be noted that the slopes of these two linear relationships are essentially the same. The straight line that represents the instantaneous efficiencies at 13:00 hours indicates a 3 to 5 percent higher efficiency as compared to the line based upon daily averages.

TABLE 5.1.--Daily Average Efficiencies

Rep.	Air-flow Rate (m^3/min./m^2) 0.32	0.48	0.53	0.64
1	0.39	0.60	0.56	0.59
2	0.37	0.52	0.56	0.72
3	0.39	0.53	0.60	0.72
4	0.40	0.57	0.55	0.73
5	0.33	0.48	0.56	0.72
Average	0.37	0.54	0.57	0.69

TABLE 5.2.--Efficiencies at 13:00 hours

Rep.	Air-flow Rate (m^3/min./m^2) 0.32	0.48	0.53	0.64
1	0.49	0.59	0.67	0.72
2	0.42	0.61	0.62	0.75
3	0.42	0.49	0.65	0.73
4	0.41	0.60	0.63	0.73
5	0.35	0.54	0.63	0.73
Average	0.41	0.56	0.64	0.74

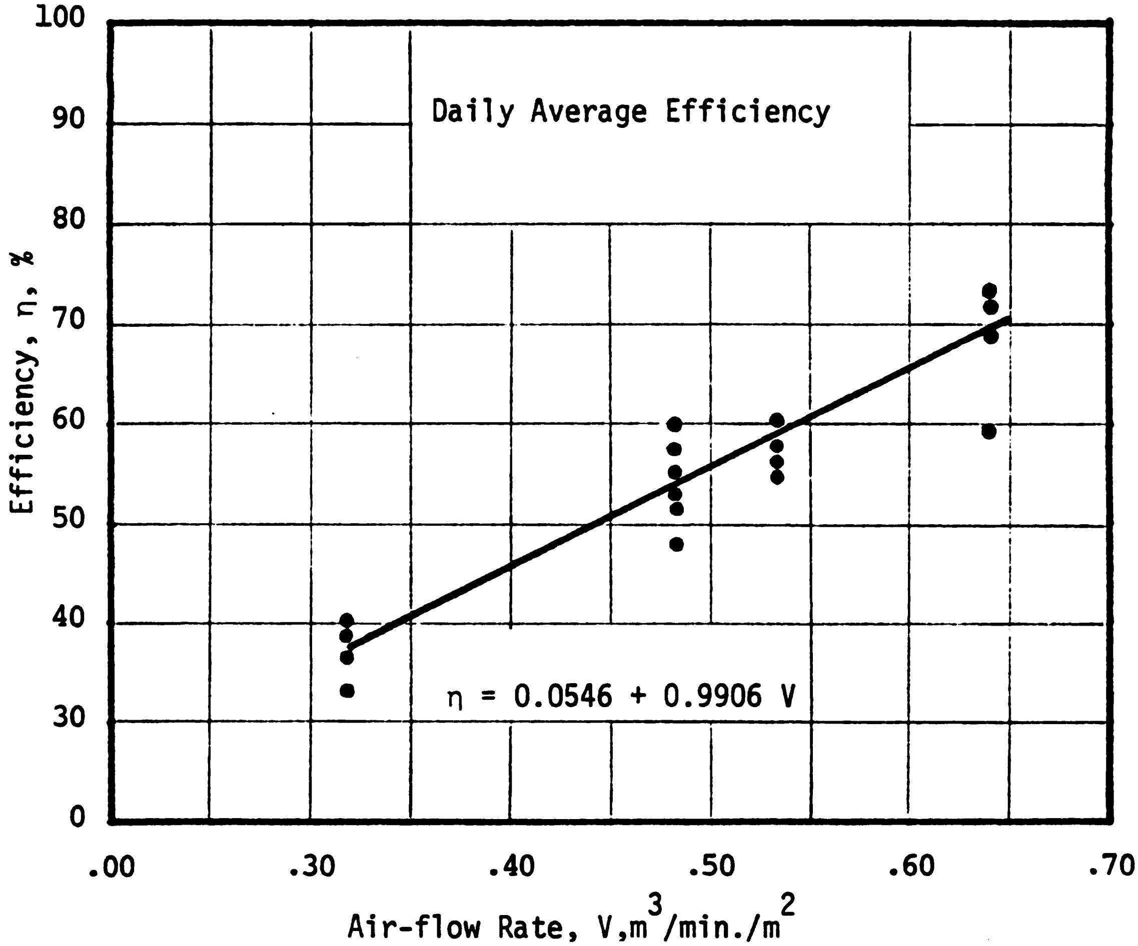

Figure 5.1.--Air-flow rate versus collector efficiency

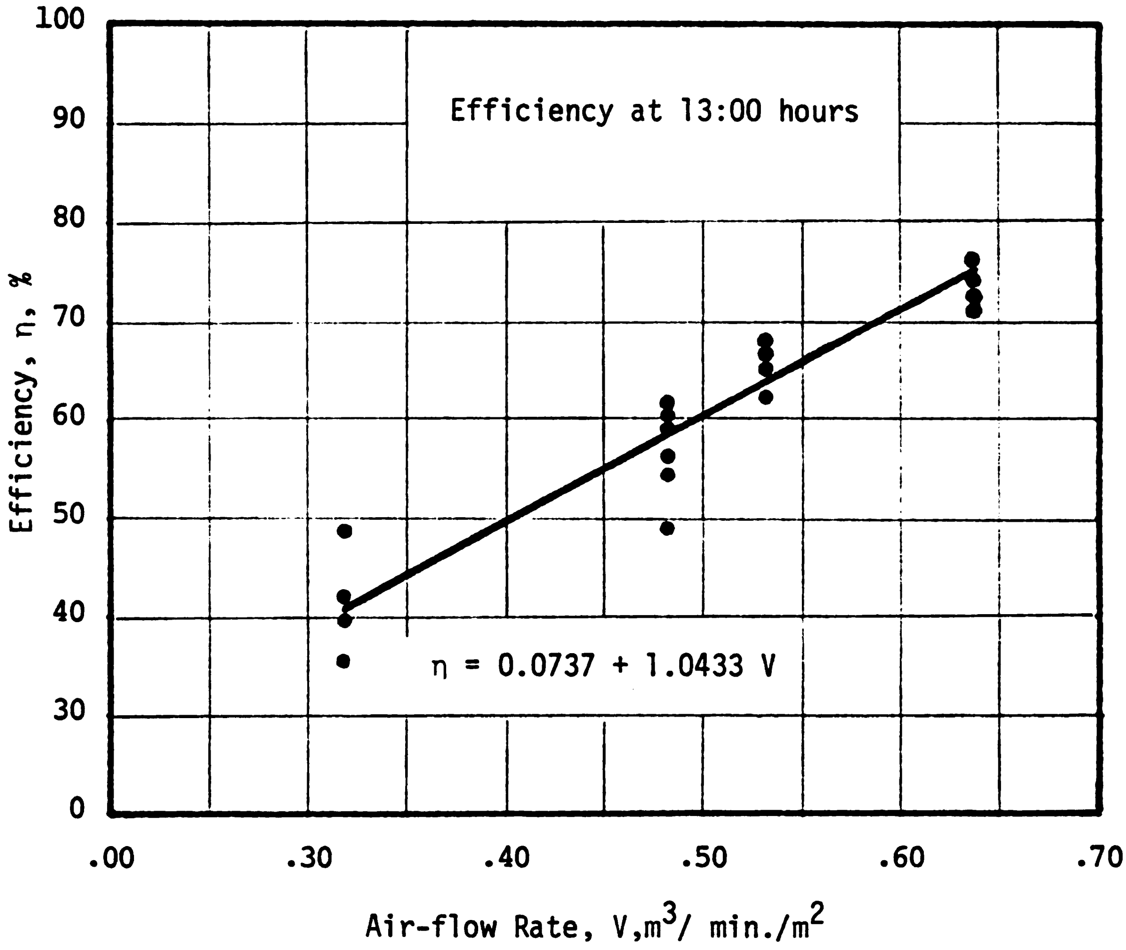

Figure 5.2.--Air-flow rate versus collector efficiency

Within the range of air flow rates observed there was essentially a direct relationship between the volumetric air flow rate and the instantaneous efficiency. Air flow rates doubled from 0.32 to 0.64 $m^3/min./m^2$ and the efficiency nearly doubled from 40 to 75 percent. This is not to infer that this relationship would continue either way beyond the limits of the air flow rates studied.

The increased solar collector efficiency with increased air flow through the collector is due mainly to the improvement in the coefficient of convective heat transfer between the absorbed plate and the air stream. This is theoretically logical as the higher velocity associated with the greater volumetric air flow produces an increased air turbulence. So as the coefficient of convective heat transfer increased, more heat was collected. If the performance measurements could have been made with all other parameters held constant, the degree of dependency of the increased efficiency on air flow rate could have been determined more reliably. Unfortunately this was not possible under operational conditions which were climatically dependent from day to day.

5.2 Collector Performance

Figures 5.3, 5.4, and 5.5 present the performance characteristics of the solar collector on three different days. Three different air flow rates, outside air temperatures, collector outlet air temperatures and absorber plate temperatures are plotted with the instantaneous efficiency values. Outside air temperatures and solar insolation varied between these three days. May 1 with the

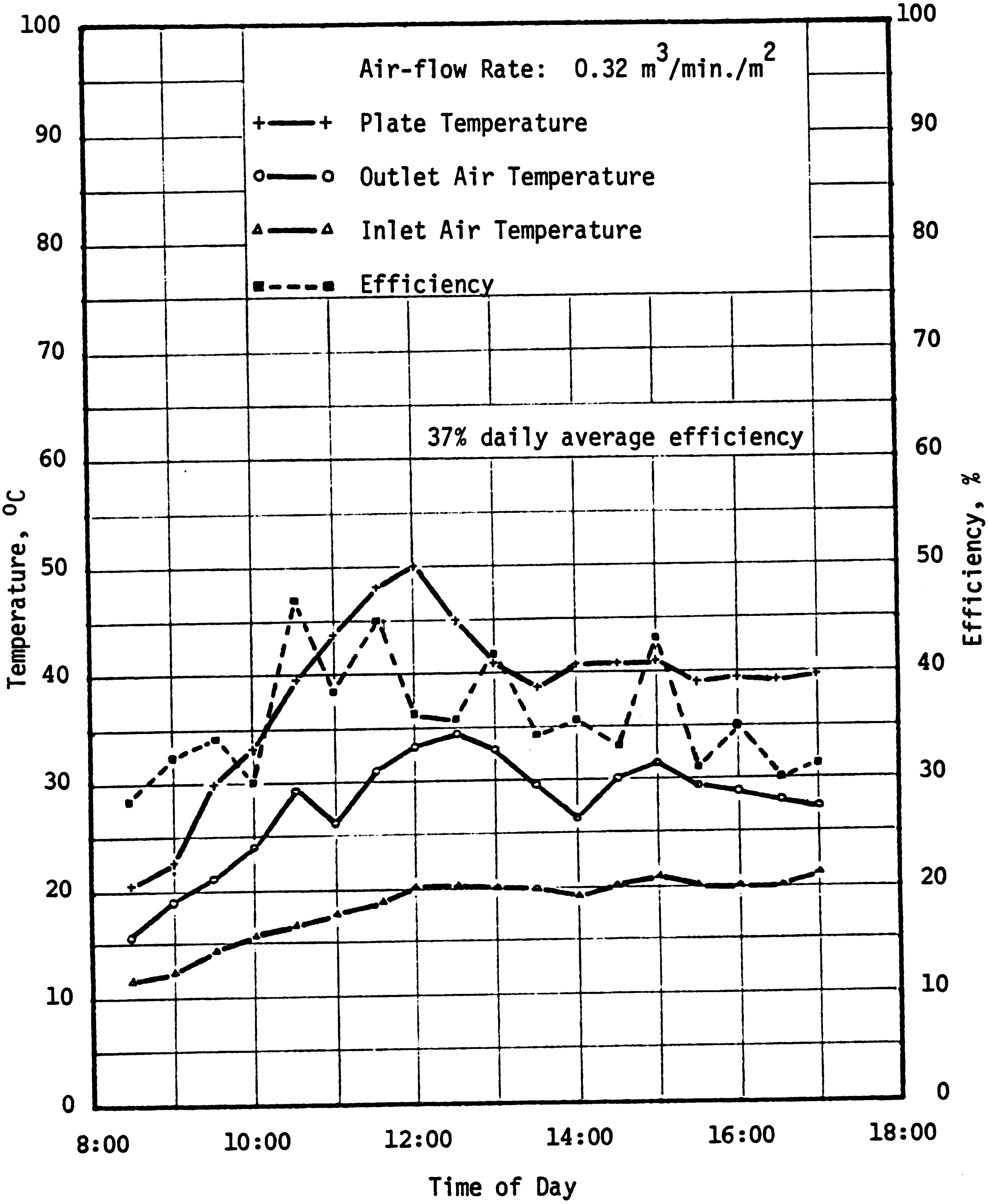

Figure 5.3.--Collector Performance, May 23, 1978

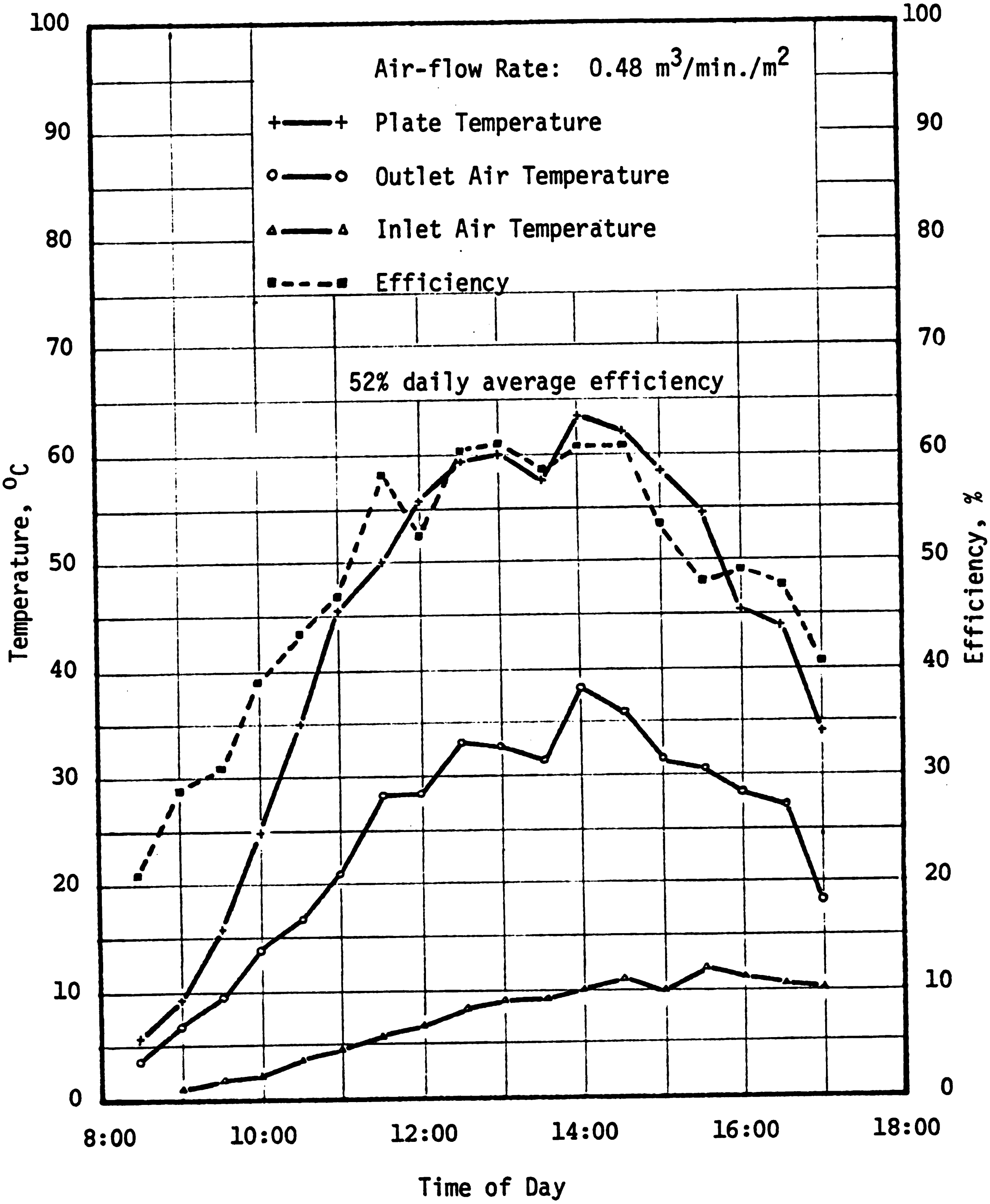

Figure 5.4.--Collector Performance, May 1, 1978

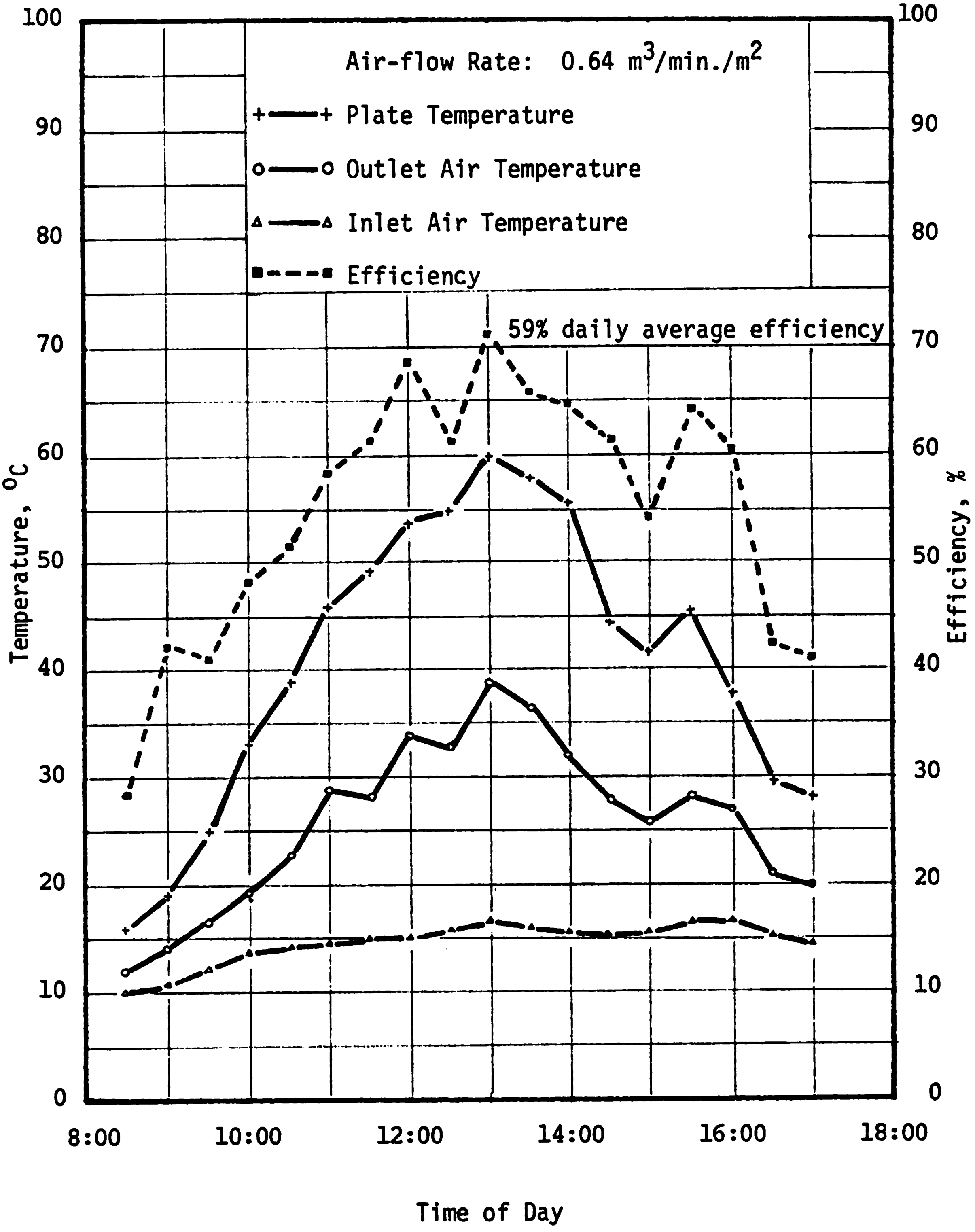

Figure 5.5.--Collector Performance, May 7, 1978

middle range of air flow was the best solar radiation, with May 7 being next, and May 23 at the slow rate the worst. The somewhat fluctuating data evident in the figures apart from experimental error, were attributed to variations in weather conditions such as variations in wind speed, wind direction, and scattered clouds.

A variation of performance efficiency throughout the days is apparent. In most all cases the efficiencies are best during the middle of the day when the insolation is highest. Figures 5.6, 5.7, and 5.8 present graphically the insolation and solar energy collected along with efficiencies for each hour of the same three days. Insolation, heat gained, plate temperatures and collector outlet air temperatures were all the lowest of the three days on the low air flow day of May 23 even though outside air temperatures were the highest. May 23 was obviously not as good a solar radiation day as May 1 and May 7 (Figures 5.4 and 5.5). It cannot be concluded though that the poor radiation day was entirely the reason for the low efficiency of 37 percent daily average for May 23 with the low air flow. The medium air flow day of May 1 (Figure 5.4) had a 52 percent daily average efficiency while the highest air flow day of May 7 (Figure 5.5) had 59 percent daily average efficiency. May 1 (Figures 5.4 and 5.7) with the middle range air flow was actually the best solar radiation day of the three but the daily average efficiency was not as high as that for May 7 (Figures 5.5 and 5.8) with the higher air flow rate.

Increased air flow rate would tend to reduce the inlet - outlet air temperature difference if there was no or just a little

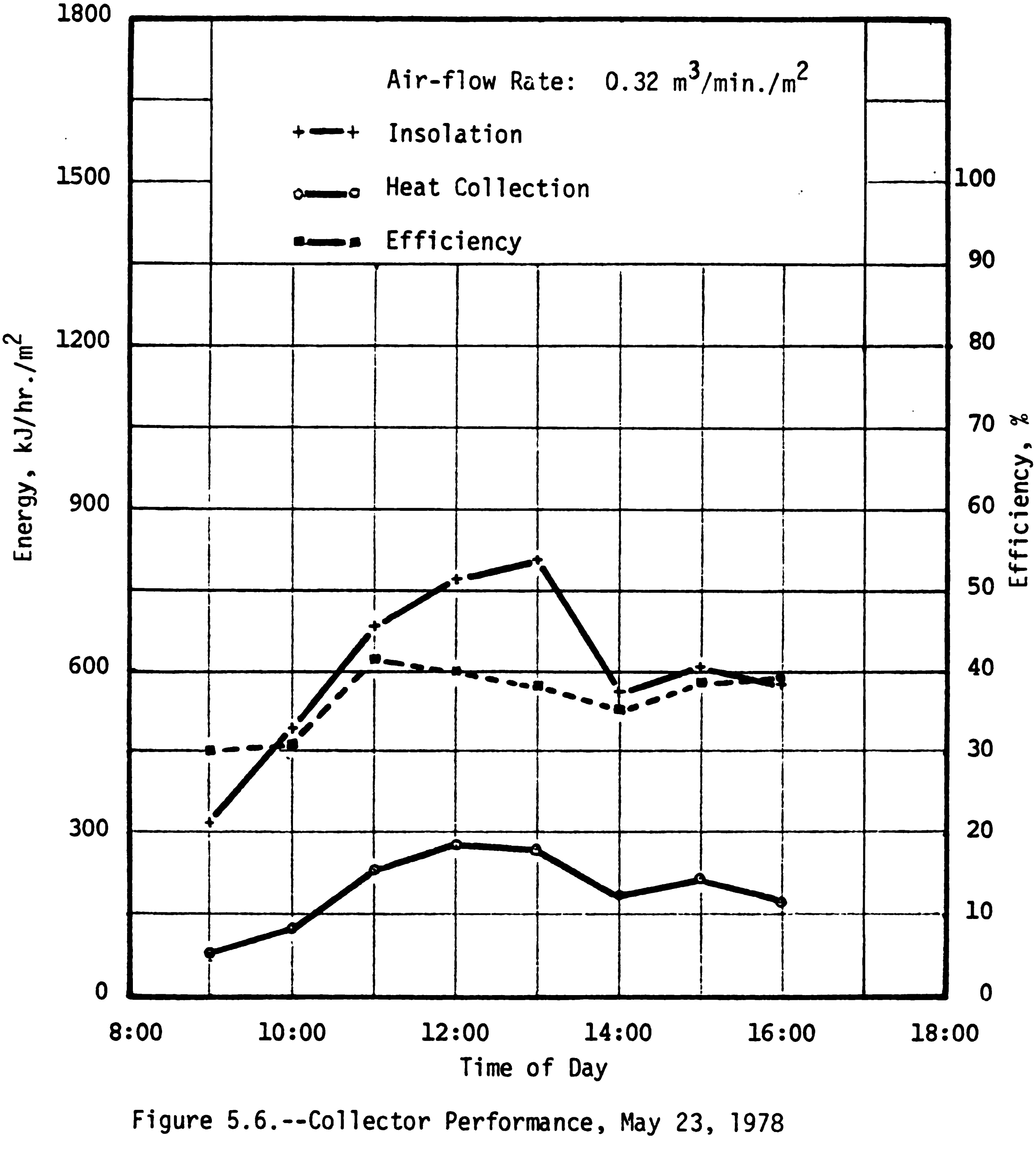

Figure 5.6.--Collector Performance, May 23, 1978

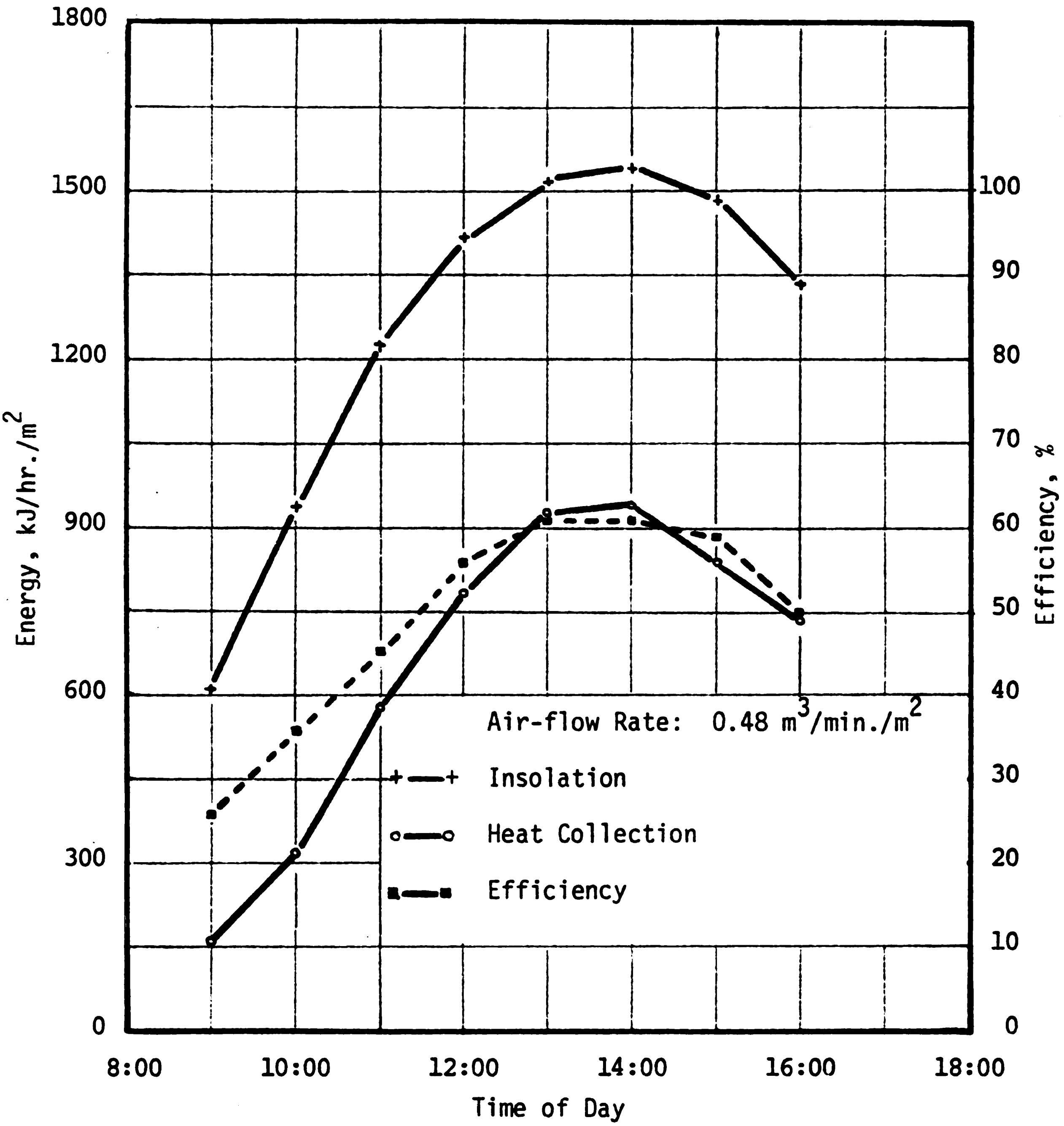

Figure 5.7.--Collector Performance, May 1, 1978

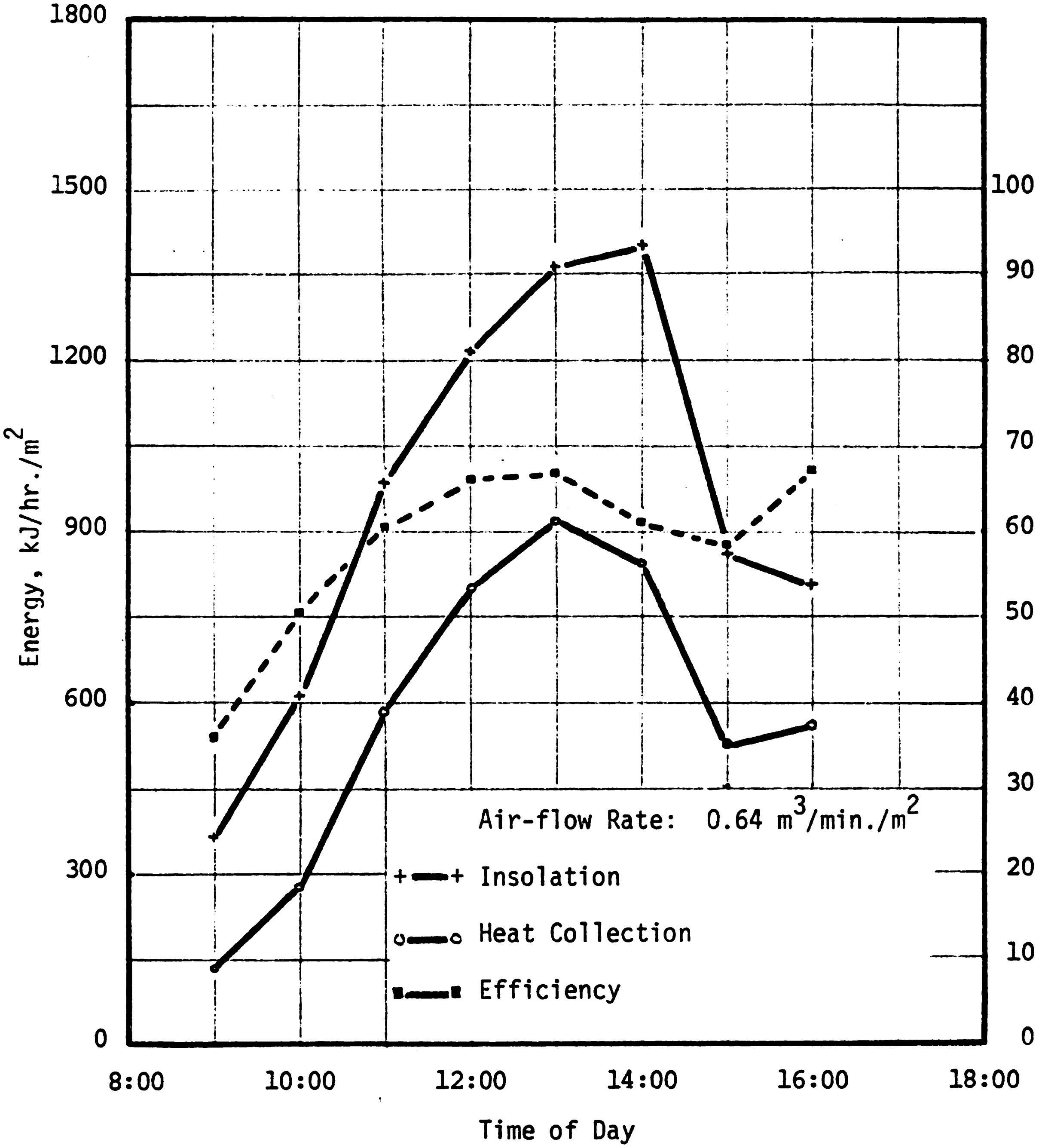

Figure 5.8.--Collector Performance, May 7, 1978

increase in the convection heat transfer coefficient, as a smaller air temperature difference would be necessary with the increased mass or volumetric air flow rate. The five observation days for each air flow rate did not show any consistant reduction in inlet - outlet air temperature differences with increased air flow rates (see Table 5.3). If anything the reverse is indicated as the average for the low air flow rate is the lowest. This undoubtedly was due to the non-similarity of the days climatically for the different air flow observations.

5.3 Solar Collector Efficiency Index

The standard methods of testing and rating solar collectors have been developed and published in the literature in order that collectors can be evaluated in a meaningful and consistent way. The standard procedure is useful especially for standardization and comparison of various designs of commercial solar collectors. The important factors which should be considered in testing and rating of the performance of plate solar collectors have been discussed in Chapter III. The flat plate solar collector efficiency can be expressed as

$$\eta = f - U_L \frac{(t_c - t_a)}{I} \tag{5.1}$$

where η = collector efficiency, percent

f = absorptance - transmittance product

U_L = overall heat loss coefficient, kJ/(hr.) (m^2) (^{o}C)

TABLE 5.3.--Average Temperature Difference (ΔT) between outlet and inlet air (^oC)

Rep.	Air-flow Rate ($m^3/min./m^2$) 0.32	0.48	0.53	0.64
1	15.03	19.37	18.26	13.21
2	8.90	19.23	17.70	19.62
3	19.25	16.99	18.57	17.60
4	20.01	16.46	-	17.99
5	16.57	16.45	-	18.21
Average	15.95	17.70	18.17	17.32

t_c = average plate temperature, ^{o}C

t_a = ambient air temperature, ^{o}C

I = insolation,

Equation (5.1) indicates that if the efficiency is plotted against the loss factor, $\frac{t_c - t_a}{I}$, a straight line will result where the slope is U_L and the y intercept is f. This equation was used to determine a thermal efficiency index for the single glass covered, air medium solar collector of this study.

A collector energy balance can be represented as

$$q_u = q_a - q_l \qquad (5.2)$$

where q_u = useful energy from the collector

q_a = available energy to the collector

q_l = energy loss from the collector

The available energy q_a is the insolation, I, multiplied by the factor f. The energy loss is

$$q_l = U_l \ (t_c - t_a) \qquad (5.3)$$

Substitution of q_l from Equation (5.2) to Equation (5.3) and by rearrangement, Equation (5.3) becomes

$$U_L = \frac{q_a - q_u}{t_c - t_a} \qquad (5.4)$$

In this study the factor f for determining q_a nor the heat loss coeffieient U_L were measurable. Some coeffieients are however available from the literature (Buelow, 1956 and Whillier, 1977). For these analyses an f value of 0.81 and a U_L of 25.95 kJ/(hr.) (m^2) (^{o}C) were assumed.. Also a true average absorber plate temperature was not measurable so Equation (5.4) was used to determine the average plate temperature from the experimental data of Table 5.4.

Figure 5.9 shows graphically the collector efficiency as compared to the collector loss factor. This efficiency plot of Figure 5.9 is representative of only one air flow rate of 0.64 m^3/min./m^2, as shown in the two right hand columns of Table 5.4.

TABLE 5.4.--Collector Performance Data at Air-flow Rate of 0.64 m^3/min./m^2

Time	T_c (°C)	T_a (°C)	$(T_c - T_a)$ (°C)→	q_u (kJ/hr./m^2)	q_a (kJ/hr./m^2)	q_l (kJ/hr./m^2)	Insol (kJ/hr./m^2)	Loss-Factor	Eff.
May 7									
9:00	16.85	10.22	6.63	140.79	312.88	172.19	386.28	0.017	0.36
10:00	21.31	12.89	8.42	278.28	496.93	218.65	613.50	0.013	0.45
11:00	22.09	14.33	7.76	588.80	790.38	201.58	875.79	0.008	0.60
12:00	21.85	14.89	6.96	805.17	984.33	179.16	1,215.23	0.006	0.66
13:00	23.61	16.56	7.05	922.25	1,105.41	183.16	1,364.71	0.005	0.67
14:00	26.74	16.67	10.07	860.55	1,121.99	261.44	1,385.18	0.007	0.61
15:00	23.73	16.67	7.06	524.25	724.07	199.82	893.92	0.008	0.58
16:00	21.29	16.89	4.40	548.40	662.70	114.30	818.15	0.005	0.67
May 19									
9:00	28.79	20.44	8.55	134.91	356.01	221.10	439.53	0.019	0.31
10:00	30.15	23.11	7.04	416.96	599.73	182.77	740.41	0.009	0.56
11:00	28.88	24.33	4.55	753.43	871.66	118.23	1,076.13	0.004	0.70
12:00	27.42	25.22	2.20	1,024.98	1,082.22	57.24	1,336.08	0.002	0.76
13:00	28.69	25.67	3.02	1,091.58	1,170.07	78.49	1,444.54	0.002	0.75
14:00	28.49	26.44	2.05	1,166.42	1,219.81	53.39	1,505.95	0.001	0.77
15:00	29.99	26.56	3.43	1,094.17	1,183.33	89.16	1,460.91	0.002	0.74
16:00	24.47	26.89	2.58	986.84	1,035.81	66.97	1,278.78	0.002	0.75

Table 5.4.--Continued

Time	T_c	T_a	$(T_c - T_a)$	q_u	q_a	q_l	Insol	Loss-Factor	Eff.
	(°C)	(°C)	(°C)→	kJ/hr./m^2					
May 22									
9:00	218.2	12.44	9.38	170.53	414.03	243.50	511.15	0.018	0.33
10:00	20.38	14.78	5.60	499.13	644.49	145.36	795.67	0.007	0.62
11:00	18.19	16.67	1.52	706.01	745.63	39.62	92.054	0.002	0.76
12:00	23.08	17.84	5.19	756.61	891.53	134.92	1,100.66	0.005	0.68
13:00	19.60	18.67	0.93	1,105.98	1,130.30	24.32	1,395.44	0.001	0.79
14:00	26.85	70.44	0.41	1,139.47	1,150.17	10.73	1,419.97	0.000	0.81
15:00	24.76	21.44	3.32	972.57	1,058.96	86.39	1,307.37	0.002	0.74
16:00	24.73	21.89	2.84	756.24	830.20	73.96	1,024.94	0.003	0.73
May 27									
9:00	26.10	21.56	4.54	211.56	329.46	117.90	406.75	0.011	0.52
10:00	30.02	24.00	6.02	362.17	518.46	156.29	640.08	0.009	0.56
11:00	26.42	25.67	0.75	737.74	747.22	19.48	934.85	0.001	0.78
12:00	28.95	26.67	2.28	912.54	976.09	63.55	1,205.06	0.002	0.76
13:00	31.66	27.67	3.99	996.68	1,100.43	103.75	1,358.56	0.003	0.73
14:00	30.27	28.22	2.05	1,078.89	1,132.27	53.38	1,397.87	0.001	0.77
15:00	33.11	29.67	3.44	1,030.92	1,120.33	89.41	1,383.13	0.002	0.74
16:00	35.05	30.78	4.27	861.81	972.77	110.96	1,200.96	0.003	0.71

TABLE 5.4.--Continued

Time	T_c (°C)	T_a (°C)	$(t_c - T_a)$ (°C)→	q_u kJ/hr./m^2	q_a	q_l	Insol	Loss-Factor	Eff.
June 9									
9:00	28.26	27.89	5.37	194.69	332.27	137.58	410.22	0.013	0.47
10:00	25.97	24.67	1.30	502.94	536.70	33.76	662.60	0.002	0.75
11:00	31.23	26.33	4.90	656.44	783.39	126.95	967.15	0.005	0.67
12:00	30.08	27.22	2.86	960.14	992.67	32.53	1,225.53	0.002	0.74
13:00	33.39	29.67	3.72	1,006.98	1,103.75	96.77	1,362.66	0.003	0.73
14:00	34.03	30.44	4.19	1,038,08	1,146.85	108.77	1,415.87	0.003	0.73
15:00	33.31	30.56	2.75	1,040.47	1,112.03	71.56	1,372.88	0.002	0.75
16:00	38.13	31.78	6.35	852.68	1,017.19	164.51	1,255.80	0.005	0.67

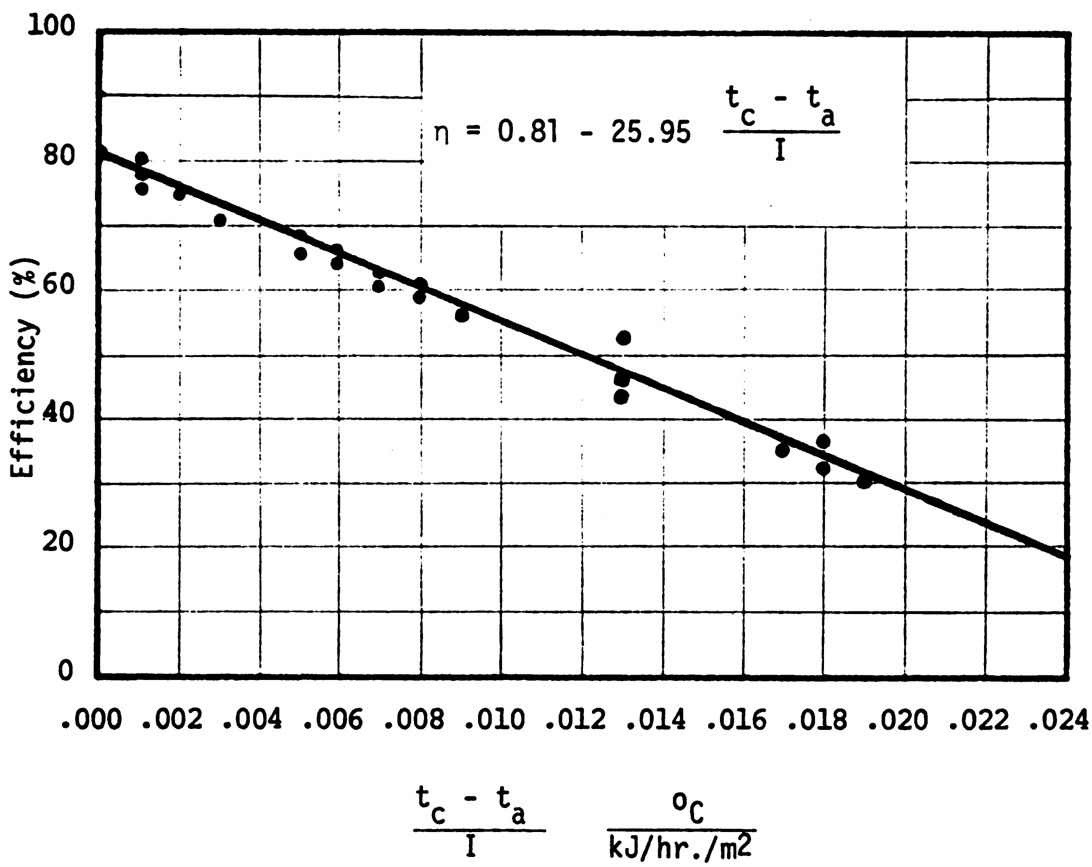

Figure 5.9.--Efficiency curve of the collector for air-flow rate of 0.64 $m^3/min./m^2$

VI. CONCLUSION

1) Within the range of air flow rates observed from 0.32 to 0.64 m^3/min./m^2, there was essentially a direct relationship between the volumetric air flow rate and the instantaneous efficiency. The collector efficiency increased linearly with increased air flow.
2) When the air flow rates doubled from 0.32 to 0.64 m^3/min./m^2 the efficiency nearly doubled from 37 to 69 percent based on daily average efficiency.
3) The daily average efficiency of the collector ranged from 33 to 73 percent and the total daily heat collection ranged from 1,949 to 7,466 kJ/m^2 depending on the air flow rate and weather conditions.
4) The maximum instantaneous efficiency of the collector was 81 percent.

BIBLIOGRAPHY

ASHRAE, 1977. Handbook of Fundamentals. Chapter 20. New York, N.Y., pp.

Baird, C. D., W. E. Waters, and D. R. Mears, 1977. Greenhouse solar Heating System Utilizing Underbench Rock Storage. A.S.A.E. paper No. 77-4012. A.S.A.E., St. Joseph, Michigan 49085.

Becker, C. F. and J. S. Boyd, 1957. Solar Radiation Availability on Surfaces in the United States as Affected by Season, Orientation, Latitude, Altitude, and Cloudiness. The Journal of Solar Science and Engineering. Vol. 1, No. 1, pp. 13-21.

Beckman, W. A., S. A. Kline, and J. A. Duffie, 1977. Solar Heating Design by the f-Chart Method. John Wiley & Sons, Inc., New York.

Bennet, I., 1965. Monthly Maps of Mean Daily Insolation for the United States. Solar Energy. Vol. 9, No. 3, pp. 145-158.

Brooks, F. A., 1936. Solar Energy and Its Use for Heating Water in California. Univ. of Calif. Agric. Exp. Sta. Bul. 602, Nov. 1936.

Brown, W. H. and R. E. Forbes, 1976. Poultry House Heating and Manure Drying Utilizing Solar Energy. Paper. Energy Research Center and Missippippi Agric. and Forestry Exp. Sta., Mississippi State University.

Buelow, F. H. and J. S. Boyd, 1955. Heating of Air with Solar Energy. Paper presented at the Annual Meeting of American Society of Agricultural Engineers, Chicago.

Buelow, F. H., 1956. The effect of various parameters on the design of solar air heaters. Thesis for the degree of Ph.D., Agricultural Engineering Department, Michigan State University, East Lansing, Michigan.

De Shazer, J. A., B. D. Moser, and N. C. Teter, 1976. Use of Solar Energy in a Modified Open Front Swine Finishing Unit. Nebraska Agric. Exp. Sta., Univ. of Nebraska - Lincoln, Nebraska.

deWinter, F., 1975. Solar Energy and the Flat Plate Collectors. An Annotated Bibliography. ASHRAE S-101. Altas Corporation, Santa Clara, California.

Duffie, J. A. and W. A. Beckman, 1974. Solar Energy Thermal Processes. John Wiley & Sons, Inc., New York.

Edwards, D. K., 1977. Solar Collector Design. The Franklin Institute Press, Philadelphia, Pennsylvania.

Elterman, L., 1967. Atmospheric Attenuation Model, 1964, in the Ultraviolet, Visible, and Infrared Regions for the Altitudes to 50 Km. Environmental Research Paper No. 46, Air Force Camb. Res. Lab.

Farber, E. A. and C. A. Morrison, 1975. Clear-Day Design Values. Applications of Solar Energy for Heating and Cooling of Buildings, Chapter IV, Edited by R. C. Jordan and B. Y. H. Liu. ASHRAE GRP 170. New York, N.Y.

Forbes, R. E. and R. W. McClendon, 1977. The Heating of a Broiler House Using Solar Energy. A.S.A.E. paper No. 77-3005. A.S.A.E., St. Joseph, Michigan 49085.

Hall, F. W., M. L. Esmay, C. Sheppard, C. Flegal, and H. C. Zindel, 1977. A Supplemental Solar Heater for Egg Production. A.S.A.E. paper No. 77-4015. A.S.A.E., St. Joseph, Michigan 49085.

Hill, J. E. and E. R. Streed, 1975. Testing and Rating of Solar Collectors. Applications of Solar Energy for Heating and Cooling of Buildings, Chapter X. Edited by R. C. Jordan and B. Y. H. Liu. ASHRAE GRP 170. ASHRAE, New York, N.Y.

Hill, J. E., E. R. Streed, and G. E. Kelly, 1976. Development of Proposed Standards for Testing Solar Collectors and Thermal Storage Devices. Technical Note 899, National Bureau of Standards, Washington, D.C.

Hill, J. E. and T. Kusuda, 1974. Method of Testing and Rating of Solar Collectors Based on Thermal Performance. National Bureau of Standards, Washington, D.C.

Horsfield, B. C. and J. DeBaerdemaeker, 1976. Drying Animal Wastes with Solar Energy. Final Report, ARS Agreement No. 12-14-7001-599, Department of Agricultural Engineering, Univ. of California, Davis, California.

Hottel, H. C. and B. B. Woertz, 1942. Performance of Flat-Plate Solar Heat Collectors. Transaction of the A.S.M.E., pp. 91-104.

Kline, G. L., 1977. Solar Collectors for Low Temperature Grain Drying A.S.A.E. paper No. 77-3007. A.S.A.E., St. Joseph, Michigan 49085.

Kondratyev, K. Y., 1969. Radiation in the Atmosphere. Academic Press, New York.

Kreider, J. F. and F. Kreith, 1975. Solar Heating and Cooling. McGraw-Hill Book Company, New York.

Liu, B. Y. H. and R. C. Jordan, 1960. The Interrelationship and Characteristic Distribution of Direct, Diffuse, and Total Solar Radiation. Solar Energy. Vol. 4, No. 3, pp. 1-19.

Lof, G. O. G. and T. D. Nivens, 1953. Heating of Air by Solar Energy. Ohio Journal of Science. 53(5): pp. 72-80.

Lof, G. O. G., 1966. World Distribution of Solar Radiation. Report No. 21, Univ. of Wisconsin Eng. Exp. Sta., Wisconsin.

Mears, D. R., W. J. Roberts, J. C. Sumpkins, and P. W. Kendall, 1977. The Rutgers Solar Heating System for Greenhouse. A.S.A.E. paper No. 77-4009. A.S.A.E., St. Joseph, Michigan 49085.

Merkel, J. A., F. C. Lewis, and J. L. Cain, 1976. Feasibility of Utilizing Solar Energy in Commercial Broiler Production. Final Report for the Period July 3, 1975 through June 30, 1976. Agric. Exp. Sta. Univ. of Maryland, Maryland.

Milburn, W. F., R. A. Aldrich, and J. W. White, 1977. Internal/External Solar Collectors for Greenhouse Heating. A.S.A.E. paper No. 77-4008. A.S.A.E., St. Joseph, Michigan 49085.

Moon, P., 1940. Proposed Standard Solar Radiation Curve for Engineering. Journal of the Franklin Institute, pp. 583-618.

Pomeranz, Y., 1978. Advances in Cereal Science and Technology. Vol. II. Association of Cereal Chemists, Inc., St. Paul, Minnesota.

Reece, F. N., 1976. Poultry House Heating and Manure Drying Utilizing Solar Energy. Final Report for Project Year July 1, 1975 to June 30, 1976. South Central Poultry Research Lab., Mississippi State, Mississippi.

Spillman, C. K., 1976. Solar Energy for Supplemental Heating of Ventilating Air for Swine Buildings. Final Report. USDA Agreement No. 12-14-7001-553. K.S.U. Project No. 5-446. Agric. Exp. Sta., Kansas State University.

Tabor, H., 1955a. Solar Energy Collector Design with Special Reference to Selective Radiation. Trans. of the Conf. on the Use of Solar Energy, the Scientific Basis. Tuscon, Arizona, Oct. 31-Nov. 1, 1955. Thermal Process, Vol. II, Part 1, Section A. pp. 1-23.

Tabor, H., 1955b. Selective Radiation. I. Wavelength Discrimination. Ibid., pp. 24-33.

Tabor, H., 1955c. Selective Radiation. II. Waterfront Discrimination. Ibid., pp. 34-39.

Tabor, H., 1958. Radiation, Convection, and Conduction Coefficients in Solar Collectors. Bull. Res. Counc. of Israel. Vol. 6c, pp. 155-176.

Tabor, H., 1962. Research on Optics of Selective Surfaces. Second Annual Report on U.S.A.F. (Camb. Res. Labs., O.A.R.) Contract AF61(052)-279, March, 1962.

Tabor, H., 1963. Research on Optics of Selective Surfaces. Final Report on U.S.A.F. Contract AF61(052)-279, May, 1963.

Tabor, H., 1977. Selective Surfaces for Solar Collectors. Applications of Solar Energy for Heating and Cooling of Buildings, Chapter VI. Edited by R. C. Jordan and B. Y. H. Liu. ASHRAE GRP 170. ASHRAE, New York, N.Y.

Tan, H. M. and W. W. S. Charters, 1970. Experimental Investigation of Forced Convection Heat Transfer. Solar Energy. Vol. 13. No. 1, p. 121.

Telkes, M. and E. Raymond, 1949. Storing Solar Heat in Chemicals. A Report of the Dover House. Heat & Vent. 46(11): 85.

Thekaekara, M. P., 1965. Survey of the Literature on the Solar Constant and the Spectral Distribution of Solar Radiant Flux. NASA SP-74.

Thekaekara, M. P., 1973. Solar Energy Outside the Earth's Atmosphere. Solar Energy. Vol. 14, No. 2., pp. 109-127.

U.S. Weather Bureau, 1964. Mean Daily Solar Radiation Monthly and Annual. Climatic Atlas of the U.S. U.S. Dept. of Commerce, U.S. Government Printing Office, Washington, D.C.

Whillier, A., 1953. Solar Energy Collection and Its Utilization for House Heating. ScD Thesis in Mech. Eng., M.I.T., 1953.

Whillier, A., 1977. Prediction of Performance of Solar Collectors. Applications of Solar Energy for Heating and Cooling of Buildings, Chapter VIII. Edited by R. C. Jordan and B. Y. H. Liu. ASHRAE GRP 170. ASHRAE, New York, N.Y.

Yellot, J. I., 1977. Solar Radiation Measurement. Applications of Solar Energy for Heating and Cooling of Buildings, Chapter III. ASHRAE GRP 170. ASHRAE, New York, N.Y.

APPENDIX

COLLECTOR PERFORMANCE DATA

Collector Performance Date on May 21, 1978

Air-flow Rate: 0.32 $m^3/min./m^2$

Time	Temperature (°C)				RH	Heat Collection	Insolation	Efficiency
	Outlet	Inlet	ΔT	Plate	(%)	(kJ/m^2/30 min.)	(kJ/m^2/30 min.)	
8:00	10.11	7.44	2.67	12.46	89	31.81	122.52	0.26
8:30	11.38	7.89	3.49	15.29	89	41.73	145.04	0.29
9:00	11.86	8.11	3.75	16.36	88	44.74	159.36	0.28
9:30	13.06	8.89	4.17	17.92	87	49.60	171.62	0.29
10:00	13.20	8.78	4.42	19.16	87	52.74	185.98	0.28
10:30	14.55	9.00	5.55	21.52	87	66.01	202.35	0.33
11:00	15.44	9.78	5.66	24.26	86	67.22	228.97	0.29
11:30	18.81	10.33	8.48	30.40	84	98.99	298.54	0.33
12:00	18.91	10.67	8.24	32.85	81	97.53	306.75	0.32
12:30	27.78	11.56	16.22	49.70	76	191.38	482.77	0.40
13:00	37.31	13.11	24.20	58.54	71	283.89	574.90	0.49
13:30	39.37	13.22	26.15	64.96	71	306.66	734.55	0.42
14:00	37.93	13.44	27.49	60.22	66	286.95	658.83	0.44
14:30	39.27	14.00	25.27	64.06	63	295.61	709.98	0.42
15:00	37.88	15.00	24.27	63.28	60	282.93	673.15	0.42
15:30	37.83	15.33	22.50	61.75	56	262.54	685.41	0.38
16:00	33.89	15.78	22.05	58.49	57	256.35	615.84	0.42
16:30	33.89	16.11	17.78	53.66	55	206.36	546.23	0.38
17:00	33.89	16.78	17.11	49.56	55	198.16	470.50	0.42
Total						3,121.29	7,850.84	

Daily Average Efficiency: 0.39

Total Daily Heat Collection: 282,788 kJ

Collector Performance Date on May 23, 1978

Air-flow Rate: 0.32 m^3/min./m^2

Time	Temperature (°C)				RH	Heat Collection	Insolation	Efficiency
	Outlet	Inlet	ΔT	Plate	(%)	(kJ/m^2/30 min.)	(kJ/m^2/30 min.)	
8:00	16.11	13.11	3.00	18.66	55	31.72	100.00	0.35
8:30	16.83	13.33	3.50	20.24	55	36.92	142.99	0.29
9:00	18.34	13.44	4.90	22.72	54	51.55	179.83	0.32
9:30	21.57	14.89	6.68	30.23	51	70.15	231.02	0.34
10:00	23.16	16.22	6.94	33.81	51	72.54	267.86	0.30
10:30	29.63	17.44	12.99	39.51	48	126.79	296.49	0.47
11:00	27.73	17.78	9.95	39.47	50	103.47	302.64	0.38
11:30	32.97	18.78	14.19	43.87	49	147.05	357.90	0.45
12:00	33.02	20.33	12.69	48.85	48	130.77	404.99	0.36
12:30	33.89	20.78	13.11	49.80	46	134.95	417.26	0.36
13:00	33.55	20.33	13.22	44.35	47	136.25	355.85	0.42
13:30	29.63	20.22	9.41	41.74	48	95.98	314.91	0.34
14:00	27.78	19.89	7.89	38.48	51	81.45	249.44	0.36
14:30	29.53	20.67	8.86	41.84	48	91.25	308.80	0.33
15:00	32.93	21.33	11.59	42.92	48	119.04	298.54	0.44
15:30	29.24	21.22	8.02	39.06	48	82.38	310.85	0.29
16:00	29.19	20.78	8.41	39.42	50	86.60	265.81	0.36
16:30	28.56	20.72	7.84	39.85	49	80.07	284.22	0.31
17:00	28.61	21.22	7.38	39.68	48	75.89	263.75	0.32
Total						1,949.04	5,253.22	

Daily Average Efficiency: 0.37

Total Daily Heat Collection: 176.583 kJ

Collector Performance Date on May 24, 1978

Air-flow Rate: 0.32 $m^3/min./m^2$

Time	Temperature (°C)				RH	Heat Collection	Insolation	Efficiency
	Outlet	Inlet	ΔT	Plate	(%)	(kJ/m^2/30 min.)	(kJ/m^2/30 min.)	
8:00	17.45	12.89	4.56	21.67	94	53.58	173.67	0.31
8:30	18.74	14.78	3.96	23.46	92	46.17	196.19	0.24
9:00	22.21	17.00	5.21	29.77	85	60.32	247.39	0.24
9:30	28.61	19.11	9.50	34.87	78	109.25	314.91	0.34
10:00	34.08	20.44	13.64	43.87	72	156.13	384.52	0.41
10:30	38.31	22.11	16.20	51.48	60	187.11	466.40	0.40
11:00	43.15	23.44	19.71	63.94	50	223.32	585.11	0.38
11:30	47.78	23.67	24.11	66.28	50	272.96	630.16	0.43
12:00	49.63	23.56	26.07	70.41	48	295.32	720.24	0.41
12:30	47.78	24.56	23.22	69.93	45	262.12	718.19	0.36
13:00	44.01	25.22	19.90	63.19	46	224.91	538.06	0.42
13:30	43.01	26.22	16.79	61.63	47	208.29	529.86	0.39
14:00	50.41	25.89	25.19	71.07	42	283.72	748.87	0.39
14:30	50.75	26,67	24.08	71.14	39	275.27	720.24	0.38
15:00	48.87	27.22	22.98	66.07	41	258.23	568.75	0.45
15:30	47.92	25.56	22.36	65.20	38	238.18	509.39	0.47
16:00	47.01	27.22	14.79	63.92	36	221.39	540.07	0.41
16:30	42.20	24.56	17.64	59.29	37	187.15	470.50	0.40
17:00	38.89	24.11	11.78	52.72	36	131.81	400.89	0.33
Total						3,689.91	9.289.82	

Daily Average Efficiency: 0.39

Total Daily Heat Collection: 334,306 kJ

Collector Performance Date on May 25, 1978

Air-flow Rate: 0.32 $m^3/min./m^2$

Time	Temperature (^oC)				RH	Heat Collection	Insolation	Efficiency
	Outlet	Inlet	ΔT	Plate	(%)	(kJ/m^2/30 min.)	(kJ/m^2/30 min.)	
8:00	18.07	15.11	2.96	19.19	86	34.49	100.00	0.34
8:30	19.45	16.56	2.89	22.75	82	33.61	177.77	0.19
9:00	22.26	18.11	4.15	28.53	78	47.80	222.82	0.21
9:30	29.24	20.00	9.24	34.32	77	105.94	282.17	0.38
10:00	33.02	21.11	11.91	40.11	62	136.00	353.80	0.38
10:30	37.88	22.00	15.88	49.25	54	180.83	437.73	0.41
11:00	42.53	22.78	19.75	56.48	53	223.49	523.71	0.43
11:30	43.58	23.22	20.36	62.39	50	230.81	583.06	0.40
12:00	46.87	24.56	22.31	66.87	46	251.87	646.52	0.39
12:30	48.82	24.78	24.04	69.56	42	271.16	671.09	0.41
13:00	51.39	26.56	24.83	71.11	38	278.36	679.30	0.41
13:30	52.17	26.44	25.73	71.21	36	288.49	687.46	0.42
14:00	53.17	26.11	27.06	71.21	34	303.69	201.82	0.43
14:30	53.73	27.11	26.62	71.83	31	297.83	707.93	0.42
15:00	52.31	27.44	24.87	21.23	31	277.86	299.77	0.40
15:30	50.70	27.89	22.81	70.22	29	254.46	652.68	0.39
16:00	48.92	28.67	20.70	67.84	30	230.64	589.22	0.39
16:30	48.35	28.33	20.02	65.12	28	219.01	511.44	0.43
17:00	44.11	28.22	15.78	60.57	26	175.68	470.50	0.37
Total						3,842.95	9,598.87	

Daily Average Efficiency: 0.40

Total Daily Heat Collection: 348,171 kJ

Collector Performance Date on June 10, 1978

Air-flow Rate: 0.32 m^3/min./m^2

Time	Temperature (°C)				RH	Heat Collection	Insolation	Efficiency
	Outlet	Inlet	ΔT	Plate	(%)	(kJ/m^2/30 min.)	(kJ/m^2/30 min.)	
8:00	19.20	16.89	2.31	21.27	53	26.79	100.00	0.29
8:30	22.40	18.44	3.96	28.02	50	45.58	214.61	0.21
9:00	28.26	20.00	8.26	31.47	47	94.68	282.17	0.34
9:30	29.14	21.00	8.14	39.39	44	92.92	347.68	0.28
10:00	33.11	21.89	11.22	45.20	40	127.79	425.46	0.30
10:30	38.70	22.67	16.03	51.86	38	182.00	517.59	0.35
11:00	39.32	23.56	15.76	56.43	38	178.49	583.06	0.31
11:30	44.11	23.67	20.44	59.39	34	231.23	636.31	0.36
12:00	43.10	24.56	18.54	62.34	34	209.21	673.15	0.31
12:30	47.40	25.22	22.18	63.05	28	249.52	691.56	0.56
13:00	47.97	25.56	22.41	64.96	28	251.91	709.98	0.35
13:30	47.92	25.78	22.14	65.17	27	248.69	716.14	0.35
14:00	46.82	25.22	23.08	64.79	27	259.69	709.98	0.37
14:30	43.20	26.44	16.76	64.70	26	240.69	697.72	0.34
15:00	43.58	26.33	20.49	62.27	24	229.72	685.41	0.34
15:30	38.41	26.78	11.63	60.90	25	183.80	634.26	0.29
16:00	38.27	26.78	11.49	56.98	23	188.07	556.48	0.34
16:30	33.40	26.33	7.07	51.93	23	176.64	478.66	0.37
17:00	33.98	26.33	7.75	36.37	23	133.78	382.47	0.35
Total						3,351.31	9,942.79	

Daily Average Efficiency: 0.33

Total Daily Heat Collection: 303,628 kJ

Collector Performance Date on June 6, 1978

Air-flow Rate: 0.48 $m^3/min./m^2$

Time	Temperature (°C)				RH	Heat Collection	Insolation	Efficiency
	Outlet	Inlet	ΔT	Plate	(%)	(kJ/m^2/30 min.)	(kJ/m^2/30 min.)	
8:00	16.58	12.67	3.91	18.59	72	69.02	100.00	0.69
8:30	18.44	15.22	3.22	22.45	64	56.21	183.93	0.30
9:00	21.74	16.56	5.18	28.05	57	90.12	222.82	0.40
9:30	23.51	17.78	5.73	31.25	55	99.20	251.49	0.39
10:00	28.65	19.22	9.43	39.63	46	162.50	339.48	0.48
10:30	32.63	19.78	12.88	42.89	43	220.97	359.95	0.61
11:00	38.27	21.44	16.83	50.15	39	287.62	450.03	0.64
11:30	43.15	22.78	20.37	57.24	34	346.72	554.43	0.62
12:00	46.87	23.78	23.09	63.05	30	351.64	630.16	0.62
12:30	48.82	24.00	24.82	64.75	30	420.69	654.73	0.64
13:00	48.94	25.11	23.83	67.58	27	402.31	685.41	0.59
13:30	50.98	25.11	25.87	68.57	24	436.76	705.88	0.62
14:00	52.72	25.67	27.05	69.77	23	455.77	709.98	0.64
14:30	53.59	26.11	27.48	70.31	21	462.30	748.87	0.62
15:00	52.76	26.78	25.98	69.35	20	436.18	712.03	0.61
15:30	48.78	27.00	21.78	66.92	18	365.22	585.11	0.62
16:00	46.87	26.56	20.31	64.04	18	365.22	552.38	0.66
16:30	42.72	27.22	15.50	59.08	20	320.98	550.33	0.60
17:00	38.31	27.11	11.20	57.64	19	262.16	501.18	0.52
Total						5,660.05	9,398.28	

Daily Average Efficiency: 0.60

Total Daily Heat Collection: 512,800 kJ

Collector Performance Date on May 1, 1978

Air-flow Rate: 0.48 $m^3/min./m^2$

Time	Temperature (^oC)				RH	Heat Collection	Insolation	Efficiency
	Outlet	Inlet	ΔT	Plate	(%)	($kJ/m^2/30$ min.)	($kJ/m^2/30$ min.)	
8:00	8.67	-1.00	9.67	5.98	56	178.82	198.24	0.90
8:30	3.39	0.33	3.06	5.77	52	56.25	263.75	0.21
9:00	6.28	1.11	5.17	9.75	50	94.85	339.48	0.28
9:30	9.68	2.33	7.35	16.83	50	134.11	433.66	0.31
10:00	13.38	2.44	10.94	25.66	49	199.67	517.59	0.39
10:30	17.20	3.56	13.65	35.57	50	248.14	581.01	0.43
11:00	21.67	4.56	17.11	45.11	49	310.05	660.88	0.47
11:30	28.22	5.78	22.44	50.41	47	404.78	703.83	0.58
12:00	28.70	7.00	21.70	55.61	44	389.84	740.71	0.53
12:30	34.03	7.78	26.25	59.41	42	470.25	779.60	0.60
13:00	34.03	8.56	25.47	60.48	39	455.06	742.76	0.61
13:30	32.92	8.67	24.25	58.70	37	433.04	730.45	0.59
14:00	38.70	10.33	28.37	64.02	35	505.53	809.99	0.62
14:30	37.35	10.78	26.57	63.05	36	471.00	755.02	0.62
15:00	33.06	10.56	22.50	58.07	36	399.26	738.66	0.54
15:30	32.63	12.00	20.63	54.59	35	364.09	757.07	0.48
16:00	28.26	12.22	16.04	45.56	37	282.93	568.70	0.50
16:30	27.68	11.67	16.01	44.85	35	282.97	579.00	0.49
17:00	19.94	10.89	9.05	34.17	36	160.44	380.42	0.42
Total						5,860.10	11,083.02	

Daily Average Efficiency: 0.52

Total Daily Heat Collection: 530,925 kJ

Collector Performance Date on May 10, 1978

Air-flow Rate: 0.48 $m^3/min./m^2$

Time	Temperature (°C)				RH	Heat Collection	Insolation	Efficiency
	Outlet	Inlet	ΔT	Plate	(%)	($kJ/m^2/30$ min.)	($kJ/m^2/30$ min.)	
8:00	15.05	9.56	5.49	21.25	85	97.78	104.10	0.93
8:30	15.37	9.78	5.59	23.16	84	99.50	251.49	0.39
9:00	15.22	10.00	5.22	20.73	80	92.80	212.56	0.43
9:30	16.49	11.22	5.27	25.14	73	93.18	237.13	0.39
10:00	21.72	12.00	9.72	36.90	67	171.58	364.05	0.47
10:30	33.45	13.33	20.12	55.82	59	353.63	603.53	0.58
11:00	28.07	13.33	14.74	49.16	58	259.02	517.59	0.50
11:30	34.37	15.00	19.37	59.41	55	337.64	720.24	0.46
12:00	37.31	15.22	22.09	62.60	56	385.69	773.44	0.49
12:30	38.75	15.78	22.97	62.08	52	400.30	736.61	0.54
13:00	39.18	17.00	22.18	64.49	58	384.94	781.65	0.49
13:30	37.31	15.89	21.42	56.22	56	373.09	619.94	0.60
14:00	33.93	15.56	17.37	53.10	47	302.06	538.06	0.56
14:30	38.22	17.11	21.11	57.05	44	366.14	664.94	0.55
15:00	38.36	17.56	20.80	53.85	40	360.37	612.95	0.58
15:30	33.98	17.56	16.42	51.22	42	284.48	540.07	0.52
16:00	33.45	17.78	15.67	45.32	41	271.25	441.83	0.61
16:30	28.22	17.78	10.44	39.61	38	180.62	355.85	0.50
17:00	-	-	-	-	-	-	-	
Total						4,814.98	8,972.85	

Daily Average Efficiency: 0.53

Total Daily Heat Collection: 436,237 kJ

Collector Performance Date on May 17, 1978

Air-flow Rate: 0.48 $m^3/min./m^2$

Time	Temperature (^oC)				RH	Heat Collection	Insolation	Efficiency
	Outlet	Inlet	ΔT	Plate	(%)	(kJ/m^2/30 min.)	(kJ/m^2/30 min.)	
8:00	14.55	10.78	3.77	17.25	91	66.89	136.84	0.48
8:30	17.13	12.22	4.91	21.94	89	86.65	177.77	0.48
9:00	19.11	14.56	4.55	25.76	83	79.70	241.23	0.33
9:30	22.65	15.89	6.76	29.63	80	117.87	284.22	0.41
10:00	28.61	17.22	11.39	36.17	74	197.57	353.80	0.55
10:30	33.45	18.22	15.23	44.66	69	263.38	433.66	0.60
11:00	37.83	19.56	18.27	52.59	62	314.74	523.71	0.60
11:30	34.08	19.89	14.19	51.62	59	244.00	548.28	0.44
12:00	42.05	20.67	21.38	60.07	57	366.81	533.96	0.68
12:30	39.23	20.89	18.34	56.03	54	314.28	607.63	0.51
13:00	38.75	21.33	17.42	58.42	54	297.95	493.02	0.60
13:30	38.27	21.00	17.27	54.49	55	295.82	372.26	0.79
14:00	42.63	22.22	20.41	64.20	50	348.10	720.24	0.48
14:30	47.49	23.00	24.49	68.35	46	416.67	724.30	0.57
15:00	48.25	23.44	24.81	67.29	67	421.48	726.35	0.58
15:30	47.78	24.44	23.34	67.93	84	395.11	701.82	0.56
16:00	29.63	20.56	9.07	37.88	82	155.67	321.06	0.48
16:30	24.07	17.67	6.40	29.21	76	110.97	128.67	0.86
17:00	32.44	19.89	12.55	42.15	70	215.95	267.86	0.80
Total						4,709.71	8,159.93	

Daily Average Efficiency: 0.57

Total Daily Heat Collection: 426,699 kJ

Collector Performance Date on June 11, 1978

Air-flow Rate: 0.48 $m^3/min./m^2$

Time	Temperature (°C)				RH	Heat Collection	Insolation	Efficiency
	Outlet	Inlet	ΔT	Plate	(%)	(kJ/m^2/30 min.)	(kJ/m^2/30 min.)	
8:00	21.27	18.78	2.49	23.46	53	43.03	100.00	0.43
8:30	22.57	19.56	3.01	26.85	51	51.90	165.51	0.31
9:00	24.44	20.78	3.66	28,05	49	62.70	200.30	0.31
9:30	29.72	21.33	8.39	33.52	47	143.49	267.86	0.53
10:00	39.92	22.67	10.25	39.03	46	174.63	335.38	0.52
10:30	33.11	22.67	10.44	45.04	45	177.90	413.20	0.43
11:00	38.84	23.56	15.28	51.34	45	259.61	499.13	0.52
11:30	39.23	23.89	15.34	56.55	42	260.11	572.85	0.45
12:00	43.96	24.33	19.63	60.19	41	332.49	621.95	0.53
12:30	44.06	25.11	18.95	63.17	38	320.06	683.36	0.46
13:00	47.78	25.11	22.67	64.37	35	382.80	701.82	0.54
13:30	47.44	26.78	20.66	65.83	32	347.06	714.08	0.48
14:00	47.87	26.89	20.98	65.88	30	352.21	724.30	0.48
14:30	47.35	27.22	20.13	65.36	27	337.14	716.14	0.47
15:00	47.92	27.33	20.59	64.13	24	344.88	718.19	0.48
15:30	48.92	28.56	20.36	64.51	24	339.86	697.72	0.48
16:00	47.78	28.33	14.45	61.49	23	324.70	662.89	0.48
16:30	43.49	29.11	14.38	58.49	21	239.43	576.95	0.41
17:00	43.58	29.11	14.47	54.82	21	241.02	505.29	0.47
Total						4,735.41	9,776.98	

Daily Average Efficiency: 0.48

Total Daily Heat Collection: 429,028 kJ

Collector Performance Date on May 7, 1978

Air-flow Rate: 0.64 $m^3/min./m^2$

Time	Temperature (°C)				RH	Heat Collection	Insolation	Efficiency
	Outlet	Inlet	ΔT	Plate	(%)	($kJ/m^2/30$ min.)	($kJ/m^2/30$ min.)	
8:00	9.60	9.00	0.60	10.73	82	14.35	145.04	0.10
8:30	12.11	10.00	2.11	15.77	76	49.93	177.77	0.28
9:00	14.05	10.22	3.83	18.08	80	90.75	208.50	0.43
9:30	16.81	12.00	4.81	25.10	70	113.23	267.86	0.42
10:00	19.92	12.89	7.03	33.11	64	165.05	346.89	0.48
10:30	23.24	13.44	9.80	39.30	58	229.39	437.73	0.52
11:00	29.72	14.33	15.39	47.82	54	359.40	538.06	0.67
11:30	29.24	14.44	14.80	49.44	53	357.90	570.80	0.63
12:00	34.08	14.89	19.19	54.45	52	447.27	646.52	0.69
12:30	34.03	15.67	18.36	55.23	49	426.88	679.30	0.63
13:00	37.93	16.56	21.37	60.52	47	495.37	685.41	0.72
13:30	37.31	15.56	20.75	59.98	46	480.84	716.14	0.67
14:00	32.97	16.67	16.30	57.10	44	377.61	669.04	0.56
14:30	28.17	16.44	11.73	45.97	44	271.75	431.61	0.63
15:00	27.63	16.67	10.96	43.70	42	253.96	462.30	0.55
15:30	29.14	16.78	12.36	47.04	41	286.23	441.83	0.65
16:00	28.82	16.89	11.43	38.41	39	262.16	422.36	0.62
16:30	22.38	16.22	6.16	30.06	39	142.78	330.81	0.43
17:00	21.54	16.00	5.54	29.77	40	128.71	307.25	0.42
Total						4,935.67	8,338.59	

Daily Average Efficiency: 0.59

Total Daily Heat Collection: 447,171 kJ

Collector Performance Date on May 19, 1978

Air-flow Rate: 0.64 m^3/min./m^2

Time	Temperature (^oC) Outlet	Inlet	ΔT	Plate	RH (%)	Heat Collection (kJ/m^2/30 min.)	Insolation (kJ/m^2/30 min.)	Efficiency
8:00	19.75	17.33	2.42	21.37	81	55.84	100.00	0.55
8:30	21.52	19.78	1.74	25.19	70	39.93	188.03	0.21
9:00	24.78	20.44	4.34	31.23	64	99.16	251.49	0.39
9:30	29.24	21.67	7.57	38.77	61	172.58	331.32	0.52
10:00	33.89	23.11	10.78	45.87	54	244.37	409.09	0.59
10:30	37.40	23.89	13.51	53.33	49	305.66	497.12	0.61
11:00	44.15	24.33	19.82	60.22	42	447.77	579.00	0.77
11:30	47.78	24.44	23.34	64.23	46	526.68	640.41	0.82
12:00	47.35	25.22	22.13	62.20	43	498.30	695.67	0.71
12:30	49.27	25.33	23.94	68.07	40	538.90	712.03	0.75
13:00	50.25	25.67	24.58	67.58	41	552.67	732.50	0.75
13:30	52.08	25.67	26.41	70.01	39	593.78	695.67	0.85
14:00	51.98	26.44	25.54	69.93	39	572.64	712.03	0.80
14:30	51.17	26.22	24.95	69.37	35	559.96	732.50	0.76
15:00	50.39	26.56	23.83	68.05	37	534.21	755.02	0.70
15:30	49.04	27.11	21.93	66.59	33	490.59	750.92	0.65
16:00	48.25	26.89	21.36	62.34	37	478.25	748.87	0.63
16:30	43.58	27.00	16.58	58.63	36	371.13	712.03	0.52
17:00	43.01	26.78	16.23	53.55	35	363.51	679.30	0.53
Total						7,446.01	10,213.58	

Daily Average Efficiency: 0.72

Total Daily Heat Collection: 674,608 kJ

Collector Performance Date on May 22, 1978

Air-flow Rate: 0.64 $m^3/min./m^2$

Time	Temperature (°C)				RH	Heat Collection	Insolation	Efficiency
	Outlet	Inlet	ΔT	Plate	(%)	(kJ/m^2/30 min.)	(kJ/m^2/30 min.)	
8:00	10.68	9.67	1.01	12.88	93	24.11	167.56	0.14
8:30	13.23	11.78	1.45	16.73	89	34.24	206.45	0.16
9:00	18.24	12.44	5.80	25.80	78	136.29	304.69	0.44
9:30	22.53	14.00	8.53	34.92	64	199.37	388.62	0.51
10:00	27.63	14.78	12.85	38.79	58	299.75	407.04	0.73
10:30	29.53	15.56	13.97	43.22	52	324.95	464.35	0.69
11:00	33.11	16.67	16.44	49.23	51	381.05	456.19	0.83
11:30	33.93	17.22	16.71	53.81	49	386.40	570.80	0.67
12:00	33.93	17.89	16.04	53.59	51	370.20	529.86	0.69
12:30	42.63	18.44	24.19	65.17	50	556.90	720.24	0.77
13:00	42.53	18.67	23.86	64.28	46	549.07	675.20	0.81
13:30	42.58	19.67	22.91	64.82	41	525.34	714.08	0.73
14:00	47.30	20.44	26.86	65.60	38	614.12	705.46	0.87
14:30	43.06	21.11	21.95	64.35	37	500.72	685.41	0.73
15:00	42.15	21.44	20.71	62.60	36	471.84	621.95	0.75
15:30	38.89	22.00	16.89	57.40	31	383.60	558.53	0.68
16:00	38.27	21.89	16.38	51.70	31	372.63	466.40	0.79
16:30	33.98	22.82	11.76	49.13	30	267.23	411.14	0.65
17:00	-	-	-	-		-	-	-
Total						5,742.98	8,886.08	

Daily Average Efficiency: 0.72

Total Daily Heat Collection: 520,314 kJ

Collector Performance Date on May 27, 1978

Air-flow Rate: 0.64 $m^3/min./m^2$

Time	Temperature (°C)				RH	Heat Collection	Insolation	Efficiency
	Outlet	Inlet	ΔT	Plate	(%)	(kJ/m^2/30 min.)	(kJ/m^2/30 min.)	
8:00	20.44	18.56	1.86	23.48	83	43.32	161.41	0.26
8:30	22.55	20.00	2.55	28.53	79	58.47	183.93	0.31
9:00	28.26	21.56	6.70	31.93	76	153.08	222.82	0.68
9:30	29.58	23.00	6.58	37.88	73	149.35	286.28	0.52
10:00	33.40	24.00	9.40	45.16	70	212.81	353.80	0.60
10:30	39.37	24.56	14.81	50.70	61	334.62	427.51	0.78
11:00	43.58	25.67	17.91	58.40	56	403.11	507.34	0.79
11:30	47.40	26.67	20.73	64.49	50	464.81	572.85	0.81
12:00	46.82	27.78	19.04	66.82	46	451.87	632.21	0.71
12:30	49.73	27.67	22.06	69.44	42	490.18	673.15	0.72
13:00	50.34	28.22	22.12	70.17	37	506.50	685.41	0.73
13:30	52.19	28.22	23.97	70.74	37	534.46	689.51	0.77
14:00	52.64	29.44	23.20	70.50	35	544.43	707.93	0.76
14:30	52.41	29.67	22.76	70.62	33	510.02	703.83	0.72
15:00	53.14	29.78	23.36	70.52	33	520.90	679.30	0.76
15:30	50.49	30.78	19.71	70.29	29	459.20	626.05	0.73
16:00	48.88	31.44	17.55	68.14	31	402.60	574.90	0.70
16:30	47.40	31.00	16.40	64.84	28	351.79	519.60	0.67
17:00	46.92	31.11	51.81	59.22	27	351.58	452.67	0.77
Total						6,943.19	9,500.62	

Daily Average Efficiency: 0.73

Total Daily Heat Collection: 629,053 kJ

Collector Performance Date on June 9, 1978

Air-flow Rate: 0.64 m^3/min./m^2

Time	Temperature (°C)				RH	Heat Collection	Insolation	Efficiency
	Outlet	Inlet	ΔT	Plate	(%)	(kJ/m^2/30 min.)	(kJ/m^2/30 min.)	
8:00	22.16	19.56	2.60	25.39	76	59.73	100.00	0.59
8:30	24.66	20.89	3.77	28.56	73	86.10	181.88	0.47
9:00	27.68	22.89	4.79	33.38	66	108.83	231.02	0.47
9:30	33.11	23.56	9.55	39.20	61	216.54	298.54	0.72
10:00	37.35	24.67	12.68	45.30	55	286.40	364.05	0.78
10:30	38.89	26.00	12.89	52.48	52	289.67	443.88	0.65
11:00	42.67	26.33	16.34	59.32	49	366.77	523.71	0.70
11:30	47.44	27.11	20.33	64.77	46	455.18	589.22	0.77
12:00	47.92	27.22	20.70	67.79	43	463.09	636.31	0.72
12:30	50.84	28.44	22.40	69.01	39	499.09	671.09	0.74
13:00	52.55	29.67	22.88	70.90	37	507.88	691.56	0.73
13:30	53.12	30.44	27.68	71.33	36	520.48	709.98	0.73
14:00	53.83	30.22	23.61	71.21	33	517.59	705.88	0.73
14:30	54.14	30.56	23.58	70.95	34	529.73	689.51	0.76
15:00	53.64	31.89	21.75	70.81	32	510.73	683.36	0.74
15:30	52.08	31.78	20.30	70.03	29	444.63	656.78	0.67
16:00	50.30	31.67	18.63	67.95	30	408.05	599.47	0.68
16:30	47.49	31.56	15.93	64.32	27	348.73	527.81	0.66
17:00	47.49	32.11	15.38	58.96	27	351.28	462.30	0.75
Total						6,970.61	9.666.43	

Daily Average Efficiency: 0.72

Total Daily Heat Collection: 631,537 kJ

Collector Performance Date on August 20, 1978

Air-flow Rate: 0.53 $m^3/min./m^2$

Time	Temperature (°C)				RH	Heat Collection	Insolation	Efficiency
	Outlet	Inlet	ΔT	Plate	(%)	(kJ/m^2/30 min.)	(kJ/m^2/30 min.)	
8:00								
8:30								
9:00	21.0	19.5	1.5		61	0.16	277.15	0.00
9:30	25.5	18.5	7.0		61	149.10	372.34	0.40
10:00	30.9	18.9	12.0		61	250.23	483.77	0.51
10:30	35.7	20.1	51.6		55	319.77	595.16	0.53
11:00	39.1	21.0	18.1		56	383.31	680.22	0.56
11:30	40.5	21.6	18.9		54	411.31	714.63	0.57
12:00	44.1	21.9	22.2		53	461.75	773.40	0.59
12:30	46.2	22.3	23.9		54	492.35	781.48	0.63
13:00	48.3	23.3	25.0		52	523.91	779.47	0.67
13:30	48.8	23.1	25.7		49	514.50	769.34	0.66
14:00	47.8	23.2	24.6		47	487.54	757.20	0.64
14:30	46.2	23.7	22.5		49	563.59	745.02	0.62
15:00	45.7	24.3	21.4		47	450.45	722.75	0.62
15:30	43.6	24.5	19.1		56	399.88	692.36	0.57
16:00	41.0	24.6	16.4		56	340.19	634.76	0.52
16:30	38.6	25.4	13.2		45	288.62	572.85	0.50
17:00	36.0	26.5	9.5		43	233.53	473.64	0.49
Total						6,161.91	10,834.62	

Daily Average Efficiency: 0.56

Total Daily Heat Collection: 558,269 kJ

Collector Performance Date on August 21, 1978

Air-flow Rate: 0.53 $m^3/min./m^2$

Time	Temperature (^oC)				RH	Heat Collection	Insolation	Efficiency
	Outlet	Inlet	ΔT	Plate	(%)	(kJ/m^2/30 min.)	(kJ/m^2/30 min.)	
8:00	14.0	15.9	-1.9		74	-	-	
8:30	18.5	18.5	0.0		70	-	-	
9:00	24.0	20.8	4.8		63	69.36	307.54	0.22
9:30	29.2	21.4	7.8		59	166.26	408.80	0.40
10:00	34.0	21.8	12.2		57	256.18	518.18	0.49
10:30	37.4	23.1	14.3		50	296.24	619.44	0.47
11:00	40.8	22.9	17.9		49	363.21	692.36	0.52
11:30	42.7	23.1	19.6		49	396.37	740.76	0.53
12:00	44.5	23.5	21.0		48	425.25	761.22	0.55
12:30	46.2	23.2	23.0		48	460.62	773.40	0.59
13:00	47.8	24.1	23.7		45	475.11	765.28	0.62
13:30	48.5	25.0	23.5		46	470.42	757.20	0.62
14:00	48.5	24.7	23.8		44	474.60	736.94	0.64
14:30	47.8	25.4	22.4		42	449.78	672.10	0.66
15:00	44.8	26.2	18.6		40	376.78	680.22	0.55
15:30	44.5	27.0	17.5		40	357.31	617.43	0.57
16:00	41.9	26.5	15.4		41	312.94	499.87	0.62
16:30	39.3	27.1	12.2		42	251.70	337.93	0.74
17:00	35.5	27.6	7.9		45	16.384	305.53	0.53
Total						5,766.04	10,194.58	

Daily Average Efficiency: 0.56

Total Daily Heat Collection: 522,403 kJ

Collector Performance Date on August 22, 1978

Air-flow Rate: 0.53 m^3/min./m^2

Time	Temperature (°C)				RH	Heat Collection	Insolation	Efficiency
	Outlet	Inlet	ΔT	Plate	(%)	(kJ/m^2/30 min.)	(kJ/m^2/30 min.)	
8:00								
8:30								
9:00	22.8	19.2	3.6		70	76.93	246.76	0.31
9:30	27.9	20.8	7.1		69	155.34	335.88	0.46
10:00	34.0	22.4	11.6		62	189.33	513.45	0.40
10:30	38.1	23.4	14.7		59	310.64	572.85	0.54
11:00	41.0	23.2	17.8		57	370.25	647.82	0.57
11:30	44.1	23.8	20.3		56	417.67	700.48	0.59
12:00	46.7	25.0	21.7		56	447.94	734.89	0.60
12:30	49.5	25.4	24.1		53	490.85	755.15	0.65
13:00	50.6	26.2	24.4		53	500.18	761.22	0.65
13:30	51.8	27.3	24.5		49	515.38	753.14	0.68
14:00	52.5	28.1	24.4		46	505.87	747.07	0.67
14:30	52.0	28.0	24.0		41	477.95	728.82	0.65
15:00	51.3	29.4	21.9		38	462.42	696.42	0.66
15:30	49.7	28.7	21.0		38	407.59	659.96	0.61
16:00	45.7	29.2	17.5		39	387.16	597.17	0.64
16:30	42.7	29.2	13.5		39	336.21	534.38	0.62
17:00	59.3	29.7	9.6		39	277.07	441.20	0.62
Total						6,328.85	10,383.20	

Daily Average Efficiency: 0.60

Total Daily Heat Collection: 573,394 kJ